Virulence shift in Type X *Toxoplasma gondii*: natural cross QTL identifies ROP33 as rodent Vir locus

KENNARD, A[1], MILLER, MA[2], KHAN, A[1*], QUINONES, M[3], MILLER, N[4], SUNDAR, N[1], JAMES, ER[5], GREENWALD, K[2], ROOS, DS[4], AND GRIGG, ME[1,5].

[1]Laboratory of Parasitic Diseases, NIAID, National Institutes of Health, Bethesda, MD, USA. [2]California Department of Fish and Wildlife, Santa Cruz, CA, USA. [3]Bioinformatics and Computational Biosciences Branch, NIAID, National Institutes of Health, Bethesda, MD, USA. [4]Department of Biology and Penn Genome Frontiers Institute, University of Pennsylvania, Philadelphia, Pennsylvania, USA. [5]Department of Medicine, University of British Columbia, Vancouver, BC, Canada.

*Current Address: Agricultural Research Service, USDA, Beltsville, MD, USA.

Abstract

How virulent parasites are maintained in nature is an important paradigm of eukaryotic pathogenesis. Here we used population genetics and molecular methods to study the evolution and emergence of genetic variants of the protozoan parasite *Toxoplasma gondii,* referred collectively as Type X (HG12), recovered from a threatened marine mammal species. Specifically, 53 *T. gondii* strains were isolated from southern sea otters (SSO) that stranded between 1998-2004 with *T. gondii* infection (ranging from chronic incidental infections to fatal encephalitis). Over 74% of these SSO, collected throughout their geographic range, were infected with Type X, based on multi-locus PCR-DNA sequencing. Depending on the locus investigated, Type X strains possessed one of three allelic types that had independently assorted across the strains examined; either genetically distinct alleles, referred to as "γ" or "δ", or a Type II allele. Phylogenetic incongruence among locus-specific trees, genome-wide CGH array and WGS analyses confirmed that Type X is a sexual clade of natural recombinants that resemble F1 progeny from a genetic cross between Type II and a mosaic of two distinct "γ" or "δ" ancestries. A single Type X genotype (19/53; 36%) that largely caused subclinical chronic infections in SSO, was highly pathogenic to mice (LD_{100}= 1 parasite). To determine whether murine virulence genes could be mapped within this population of natural isolates, we performed a genome scan and identified four QTLs with LOD scores greater than 4.0. Targeted disruption of ROP33, the strongest candidate from among 16 genes within the highest QTL on Chromosome VIIa established ROP33 as a murine virulence locus. The ability of this highly pathogenic mouse-virulent *T. gondii* clone to expand its environmental niche and infect a majority of SSO supports a virulence shift model whereby generalist pathogens like *T. gondii* utilize their sexual cycles to produce new strains that possess an expanded biological potential. Such a trait enables pathogens to extend their host range or be naturally selected within their vast intermediate host range to maximize transmission. Our work establishes a rationale for how virulent strains can be maintained cryptically in nature across a pathogen's broad host range, and act as potential reservoirs for epidemic disease.

Importance

Waterborne outbreaks of protozoal parasites are capable of causing fatal disease in a wide range of animals, including humans. Population expansion of felids in addition to anthropogenic changes near marine estuarine environments may facilitate marine wildlife exposure to highly infectious *Toxoplasma gondii* oocysts shed in felid feces. Infected cats

shed millions of environmentally-resistant *T. gondii* oocysts that can be widely dispersed by storm events. In North America *T. gondii* is thought to possess a highly clonal population structure dominated by 4 clonal lineages (I, II, III, and X). Population genetic analysis of 53 *T. gondii* isolates collected longitudinally from SSO infected with *T. gondii* that stranded between 1998-2004 identified 74% of otters infected with Type X *T. gondii*, and that Type X is not a clonal lineage, but rather a recombinant clade of at least 12 distinct strains consistent with a recent genetic cross. Importantly, one Type X haplotype was isolated from 36% of southern sea otters (*Enhydra lutris neries*) across their geographic range in California. This haplotype was highly pathogenic to mice but caused relatively benign infections in SSO. A genome scan was performed to identify a virulence locus; a secreted serine threonine kinase (ROP33) that enhanced pathogenicity in laboratory mice, but not sea otters. Our data support a virulence shift model whereby generalist pathogens like *T. gondii* utilize their sexual cycles to produce virulent strains that can be maintained cryptically in nature, according to their differential capacity to cause disease within the pathogen's broad intermediate host range. This type of "host selection" has important public health implications. Strains capable of causing fatal infections can persist in nature by circulating as chronic infections in resistant intermediate host species that act as reservoirs for epidemic disease.

Introduction

How successful microbes maintain reservoirs of virulent strains in nature is understudied and is an important paradigm of infectious disease. Whereas many studies document how microbial pathogens acquire or admix genetic material to influence their pathogenicity, relatively less is known how emergent strains of varying pathogenicity are selectively maintained in nature. Viruses can undergo reassortment to rapidly produce admixture lines that possess a range of altered biological potential, including virulence [1]. Bacteria can transfer mobile plasmid elements that encode pathogenicity islands via conjugation, conferring an altered virulence potential to recipients [2-4]. Among fungi and protozoa, genomic variation can be generated by genetic hybridization and produce novel admixture lines capable of causing disease outbreaks or altering host range [5-7]. Less clear are the mechanisms that allow highly prevalent pathogens to maintain virulent strains cryptically in nature. We sought to test whether generalist pathogens, such as the protozoan parasite *T. gondii* can leverage its broad range of intermediate hosts to selectively partition parasite genotypic diversity and virulence potential.

Toxoplasma gondii is a highly successful and prevalent protozoan pathogen that infects diverse wildlife, livestock, and 20-80% of humans worldwide [8-10]. This parasite's success in nature is largely attributed to its highly flexible life cycle. It is propagated asexually after ingestion of tissue cysts or sporulated oocysts among essentially all warm-blooded vertebrates. It can also propagate sexually within its definitive felid host by self-mating (when a single genotype undergoes fertilization and sexually clones itself) or by out-crossing (producing as many as 10^8 genetic hybrids that are transmissible as environmentally stable, highly infectious oocysts). Genetic hybridization has been shown to produce genotypes that possess a wide spectrum of biological potential, including altered virulence or a capacity to expand as successful epidemic clones [7, 11, 12]. Importantly, the broad spectrum of disease states caused by these admixture clones is highly dependent on both parasite genetics and host animal species [8, 13-15]. In rodents, low dose inocula of recombinant Type I *T. gondii*

strains are uniformly lethal to laboratory mice [16], whereas Type II strains are considerably less virulent and routinely establish chronic infections that are transmissible to other hosts [14]. In contrast, wild-derived CIM mice possess resistant alleles of immunity-related GTPases (IRGs), which inactivate parasite virulence-associated secreted kinases (ROP18/ROP5) and render mice resistant to *T. gondii* infection, including virulent Type I strains [17, 18]. Likewise, some laboratory rat strains and species are resistant to Type I infections and fail to transmit parasites [19]. The molecular basis for rat resistance is an allele-dependent activation of the NLRP1 inflammasome that results in macrophage pyroptosis and inhibition of parasite growth in Lewis (LEW) and Sprague Dawley (SD) rats, but not Brown Norway (BN) or Fischer CDF rats, which go on to establish chronic, transmissible infections of mouse-virulent Type I strains [20-22]. The result of this host-parasite genetic interplay determines the potential for a disease-producing virulent clone to cause either a non-transmissible infection or be maintained cryptically in a strain-specific, or host species-specific manner. While laboratory studies suggest that virulent strains can be maintained cryptically across the pathogen's host range [23], this phenomenon has not been fully investigated, nor has it been demonstrated to occur in a natural setting.

Between 1998 and 2004, *T. gondii* was reported as a significant cause of morbidity and mortality in southern sea otters (*Enhydra lutris nereis*), a federally listed threatened species [24, 25]. Detailed necropsy and histopathology studies identified a wide spectrum of outcomes among *T. gondii*-infected sea otters, ranging from chronic asymptomatic infections to fatal systemic disease [25, 26]. Prior studies also suggested that most southern sea otters were infected by a single outbreak clone, referred to as Type X (or HG12) [25]. Based on multi-locus PCR-DNA sequencing (MLST) using a limited set of genotyping markers, Type X was defined as the fourth clonal lineage in the US [27] and was highly prevalent in sylvatic niches, representing 47% of chronic, subclinical, or mild *T. gondii* infections in examined US wildlife [28, 29]. However, the broad range of post-infection outcomes observed in stranded southern sea otters was not consistent with infection by a single clone. Other possibilities proposed to explain this variation in disease susceptibility included co-infection [30], and exposure to immune-suppressive environmental pollutants, or toxins [31]. More recently, whole genome sequencing (WGS) performed on 62 globally-distributed *T. gondii* isolates suggested that MLST analyses may not be sufficiently resolved to predict clonotypes because they survey only limited genetic heterogeneity [15]. Although a previous study concluded that Type X was comprised of two genotypes [32], these two genotypes differed by only a few SNPs, so it was not clear whether strain variation was contributing to sea otter disease outcome in this novel host-parasite interaction.

To further investigate the extent of genetic diversity among naturally circulating Type X isolates, we sequenced a wide selection of linked and unlinked markers across the nuclear and organellar genomes for 53 *T. gondii* isolates collected longitudinally from southern sea otters that stranded in California, USA from 1998 through 2004. Based on initial genotyping results, we selected 14 sequence-confirmed Type X isolates for WGS. Analysis of our data support a model whereby Type X exists as a recombinant clade of strains that resemble F1 progeny from a natural cross between a Type II strain and a novel genotype that has not been identified previously in nature. We show that one Type X genotype was widely distributed in southern sea otters and caused the majority of *T. gondii* infections, which were largely subclinical in sea otters. This same genotype was highly pathogenic to laboratory mice, and a population level, forward genetic approach using WGS mapped a mouse virulence gene to

140 a novel parasite-specific secreted kinase ROP33, also referred to as WNG3 [33]. Our data
141 suggest that *T. gondii* can leverage its broad range of intermediate host species to partition
142 its genetic diversity such that infected hosts play a central role in the selection, expansion,
143 and maintenance of cryptically virulent *T. gondii* strains. In effect, these infected hosts act as
144 reservoirs that have the potential to cause epizootics or epidemics in other host species.
145
146 **Results**
147
148 **Genetic characterization and pathogenesis of *T. gondii* strains isolated from southern**
149 **sea otters**
150 During the sample period (1998-2004), pathological examinations carried out on
151 southern sea otters that stranded along the California coast identified numerous systemic
152 protozoal infections caused by *T. gondii, Sarcocystis neurona*, or co-infection with both
153 parasites [25, 29, 32, 34]. A primary goal of this study was to determine if *T. gondii*-associated
154 sea otter mortality was dependent, at least in part, by the protozoal genotype causing
155 infection. In total, 53 *T. gondii* isolates collected longitudinally from 1998 through 2004 from
156 minimally decomposed, stranded southern sea otters were included in this study. Isolates
157 were obtained throughout the sea otter range along the central California coast
158 (Supplemental Figure 1). For nearly all isolates (n=52), sea otter IFAT titers, stranding
159 locations, sex, and *S. neurona* co-infection status was available. Among 53 sea otters
160 examined, *T. gondii* was considered the primary cause of death among 8 animals (15%), a
161 contributing cause of death among 11 sea otters (21%) and determined to have caused
162 incidental, relatively benign infections in the remaining 34 sea otters (64%) (Supplemental
163 Figure 1).
164 Initial genetic analysis performed on a subset of 35 sea otter *T. gondii* isolates
165 established that 21 were a new genetic type, referred to as Type X (also known as
166 Haplogroup 12, or HG12), but this conclusion was limited to sequence typing at a single
167 locus, GRA6 [25]. Hence, we developed a multi-locus (MLST) PCR-DNA sequence-based
168 typing scheme using 4 additional unlinked markers (BSR4, BAG1, SAG3, and ROP1) that
169 possess a wide-range of phylogenetic strength, including markers under neutral (BSR4),
170 diversifying (GRA6, SAG3, ROP1), and purifying (BAG1) selection to determine the *T. gondii*
171 genotypes that caused infection among 53 sea otter *T. gondii* isolates. Typing solely at the
172 GRA6 marker identified three sequence types, either a Type II allele in 16 (30%) isolates, or
173 two non-archetypal alleles, previously identified as X or A [25, 32], in 25 (47%) and 12 (23%)
174 isolates, respectively. Expanding the genetic analysis across the five markers showed that 2
175 of 16 isolates with a Type II allele at GRA6 were predicted to be non-Type II recombinant
176 strains, because they possessed non-archetypal alleles at ROP1 (sea otter 3675) or BSR4 and
177 BAG1 (sea otter 3671) (Figure 1A).
178
179 **Possible point-source exposure of Type II *T. gondii* strains in southern sea otters**
180 In total, fourteen otters were infected by Type II strains because they possessed only
181 Type II alleles at all 5 assessed loci, including 12 (86%) otters that stranded within a 28 km
182 span from Moss Landing to Monterey Bay; this discreet clustering of Type II *T. gondii*-
183 infected sea otters is suggestive of regional or point source exposure. The other two Type II-
184 infected otters were recovered from Pismo Beach, approximately 282 km south of the
185 potential region of point source exposure. Although most Type II-infected otters (9/14;

64%) were collected during the first half of the study (Supplemental Figure 1B), due to the small sample size, this could be due to random chance. In our sample of 14 Type II *T. gondii* strains, more male sea otters were infected than females (11 vs. 3, respectively), and males were shown to be at significantly higher risk for Type II *T. gondii* infection, when compared with all other strains via a Fisher's two-sided exact test (p=0.028). In mice, Type II strains are considered subclinical or avirulent because they require high dose infections, immunosuppression, or mutations that affect host immune signaling pathways in order to cause mortality [14]. In sea otters, infection with Type II strains was generally incidental, with only 1/14 (7%) sea otters succumbing to *T. gondii* infection as a primary cause of death (Supplemental Figure 1).

Type X is a recombinant clade of strains and pathogenicity is dependent on haplotype

Of the remaining 39 (74%) *T. gondii* isolates, a maximum of just three alleles was identified at the 5 sequenced loci: either a canonical Type II allele or one of two genetically distinct alleles, referred to as "γ" or "δ", that appeared to segregate independently across the isolates (Figure 1A). In total 8 distinct haplotypes, designated A-H, were resolved based on their differential inheritance of the limited alleles, consistent with recombination between a Type II strain and a mosaic of two distinct ancestries as the most plausible explanation for the genetic relationship among the non-Type II strains. The Type X haplotype designated A was most common (19/39; 49%); was widely distributed across the entire southern sea otter range (Supplemental Figure 1), and was isolated from sea otters stranding every year except 2000. Infection with haplotype A, in similar to Type II infection, was likewise generally incidental, with only 1/19 (5%) haplotype A sea otters succumbing to *T. gondii* infection as the primary cause of death (Supplemental Figure 1). Another sea otter infected with haplotype A *T. gondii* that died acutely was co-infected with *Sarcocystis neurona*, and it was not possible to differentiate the relative contribution between both parasites in relation to the cause of death. In addition, although our sample size was small and thus not definitive, most of the Type X haplotype A isolates (14/19) were collected in the last 3 years of the study, which may suggest that this genotype expanded relative to other genotypes across the seven year study. In addition, Type X haplotype A strains represented the majority of sea otter *T. gondii* infections that yielded isolates (8/9) in 2003 (Figure 1B). Conversely, infection of sea otters with *T. gondii* Type X haplotype F (3/3) was highly pathogenic; these otters were significantly more at risk from fatal toxoplasmosis, compared to otters infected with haplotype A (Fisher's two-sided exact test [p=0.036])

Acute virulence in mice is dependent on Type X haplotype

Linking mortality in sea otters to *T. gondii* genotype in a wild animal population is particularly challenging given the many confounding variables that may influence disease outcome, including exposure to chemical pollutants, immunosuppression, or co-infection with other pathogens such as *S. neurona*. In contrast, studies using peritoneal infection models of *T. gondii* in laboratory mice have been instrumental in identifying causal linkages between *T. gondii* genotype and virulence. Using an inoculum of 50 parasites, mouse avirulent strains (*e.g.,* Type II) establish chronic, transmissible infections, whereas mouse virulent strains (*e.g.,* Type I) die acutely within 10-14 days [7].

Among the sea otter *T. gondii* isolates, three mouse virulence phenotypes were identified: virulent (red; all mice died acutely), intermediate virulent (blue; some mice

232 survived acute disease), and avirulent (green; all mice survived acute infection and became
233 chronically infected). The two otter isolates that possessed a Type II MLST (2987, 3131)
234 were avirulent (Figure 1C; green) and phenocopied the infection kinetics of two well studied
235 Type II lines; Me49 and 76K. Among the Type X haplotypes, E and G were also avirulent.
236 Three otter isolates from haplotype A, the genotype associated with most infections in
237 sampled sea otters, were highly pathogenic to mice; all infected mice died acutely (Figure
238 1C; red). Haplotypes D and H were likewise highly virulent in mice. The three haplotype F
239 otter isolates all possessed an intermediate virulence phenotype (Figure 1C; blue).
240 Interestingly, the virulence phenotypes for the 5 isolates from haplotypes B and C were
241 mixed, either avirulent (green) or intermediate virulent (blue) (Figure 1C). Because the Type
242 X isolates displayed a range of virulence phenotypes, our data suggest that the Type X group
243 represents a clade of recombinants from a genetic admixture of a mouse avirulent Type II
244 strain and at least one other parent that is mouse virulent, rather than expansion of a single
245 clonal lineage. In addition, not all isolates within each subgroup displayed equivalent
246 virulence kinetics; isolates from the B and C haplotypes were either avirulent or possessed
247 intermediate virulence, suggesting that the 5 marker MLST was insufficiently resolved to
248 capture the full range of genetic and phenotypic diversity of *T. gondii* isolates infecting SSO.
249 To explore this possibility, 21 isolates (18 isolates assayed through mice plus 3
250 additional isolates, one each from haplotypes A, C and D), were further genotyped using 18
251 genetic markers (17 nuclear-encoded single copy gene loci plus one microsatellite marker),
252 representing an expanded set of linked and unlinked loci across the genome. Two additional
253 markers, one each from the organellar genomes of the apicoplast and mitochondria, were
254 also included to determine the ancestry of each maternally inherited genome. This
255 represented a significant increase in the number of markers (n = 20), when compared with
256 those used to conclude that Type X (HG12) is a clonal lineage [10, 27, 35]. This 20 marker
257 MLST method provided 15,404 bp of sequence information to determine the genetic
258 relationship among *T. gondii* strains isolated from SSO (Supplemental Table 1).
259
260 **Type X is comprised of 12 distinct haplotypes by an expanded MLST analysis**
261 To establish the number of haplotypes among the 21 isolates described in the
262 previous section, sequence data for the 17 nuclear-encoded single copy gene loci was
263 concatenated and analyzed using eBURST (Figure 1D). eBURST resolves strains into clonal
264 complexes (CC) that are in linkage disequilibrium. In this case, alleles at each locus were
265 numerically coded and their inheritance pattern used to group strains that were identical
266 from those that differed at one locus (or share 16 out of 17 markers); isolates that differed
267 at the same genetic locus were grouped together, isolates that differed at a separate locus
268 were connected by a line within each clonal complex. As expected, eBURST clustered the two
269 Type II isolates (2987, 3131) into a single clonal complex with Me49 (CC1). Type X subgroup
270 G isolate 3675, originally identified by its allele at the microsatellite marker ROP1, was
271 included within CC1 because it differed from Type II strains at only SAG4. For the remaining
272 18 Type X isolates, 15 clustered into 3 clonal complexes (designated CC2-CC4), and 3 unique
273 haplotypes (3671, 3819, 4166) were resolved. The eBURST analysis failed to support a clonal
274 lineage designation for Type X. Further, the increased resolution provided by the 17 markers
275 subdivided the 8 distinct haplotypes defined using 5 loci in Figure 1A into 12 haplotypes
276 (Figure 1D) which was consistent with another study that resolved Type X *T. gondii*
277 genotypes isolated from southern sea otters into 8 genotypes [26]. One isolate each, from

278 subgroups A (n=4; 3168), C (n=4; 3160), D (n=3; 4166) and F (n=3; 3387), was resolved
279 further as unique haplotypes based on the inheritance pattern of alleles at PK1, SAG4 and
280 GRA7 (Supplemental Table 1).
281
282 **Type X resembles a recombinant clade of F1 progeny from a natural cross**
283 eBURST is insufficiently resolved to distinguish among isolates that exist either as
284 variants within a clonal lineage (because they possess alleles that differ by only minor
285 mutational drift), or as genetic admixtures that possess genetically distinct alleles derived
286 from different parental types. Previous studies suggested that Type X (or HG12) is a clonal
287 lineage infecting sea otters and wildlife in North America, and that HG12 represents an
288 expanded clone from a sexual cross between a Type II strain and a new genetic lineage that
289 was referred to as "γ"; however this conclusion was based largely on alleles found at just a
290 few loci, including GRA6 and GRA7 [24, 25, 27]. To investigate whether the genetic
291 relationship among the 12 distinct haplotypes is supported by models of genetic drift or
292 recombination, individual maximum likelihood trees were created for each of the 17 nuclear-
293 encoded single copy gene loci, the microsatellite locus, and the two organellar loci
294 (Supplemental Figure 1). To distinguish between alleles undergoing minor mutational drift
295 and those that have evolved independently as distinct genetic outgroups, 1000 bootstrap
296 replicates were run for each tree, with supported nodes above 60% indicated at each marker.
297 For each tree, the 19 isolates identified as Type X were labeled in purple, and isolates
298 belonging to the clonal lineage I (n=1), II (n=3), and III (n=1) were labeled in red, green, and
299 blue respectively (Figure 2).
300 At 5 genetic markers located on chromosomes Ib, II, III, XI, and XII, all 12 distinct Type
301 X haplotypes possessed a canonical Type II allele (green), with no minor mutational drift
302 detected, consistent with Type II being one of the parental genetic backgrounds
303 (Supplemental Table 1). At the L358 marker on chromosome V, however, all Type X isolates
304 except 3675 possessed a Type I or "α" allele (red), indicating the presence of mixed ancestry.
305 Further, at the BSR4 marker on chromosome IV, all Type X isolates except 3675 possessed
306 an entirely novel allele that was readily differentiated from Type I, II and III strains with
307 strong bootstrap support (Figure 2B). At all remaining loci, Type X isolates possessed either
308 a Type II or one of 2 genetically distinct alleles, which could not be readily explained by minor
309 mutational drift. Hence, across all 17 nuclear-encoded markers, each isolate possessed either
310 a Type II allele, or an allele of distinct ancestry that was referred to as belonging to "α" (red),
311 "γ" (purple) or "δ" (orange) lineages.
312 The maternally inherited organellar genome markers were likewise mixed. At the
313 mitochondrial marker CO1, two alleles were identified, either an allele common to Type I, II
314 and III strains or a novel allele designated "γ" (Figure 2A). Further, 3 distinct alleles were
315 identified at the apicoplast marker APICO: a Type I or "α" allele (red), a Type II allele (green)
316 or a novel "γ" allele (purple), supporting the mixed ancestry designation. Each of the 12 Type
317 X haplotypes were therefore a mosaic of mixed ancestry that possessed some combination
318 of Type II, Type I, "γ" or "δ" alleles that had segregated independently across all loci
319 investigated. The data are consistent with Type X existing as a recombinant clade resembling
320 F1 progeny that was recently derived, without sufficient time to develop minor mutational
321 drift (Supplemental Table 1).

322 In support of the sexual cross model, incongruity between phylogenies for each
323 haplotype was readily observed between markers located in different portions of the
324 genome. In Figure 2C, 8 isolates shared the same ancestry between the two genetic loci
325 located on separate chromosomes VIIa and VIIb (GRA7 and BAG1 respectively); these
326 variations were shaded either green (Type II alleles at both loci) or purple (γ lineage alleles
327 at both loci). In contrast, 13 isolates had independently segregated chromosomes of mixed
328 ancestry, indicated by orange and pink coloration to depict isolates that were discordant and
329 possessed different ancestral alleles at each locus; the crossing of orange and pink lines
330 highlights this incongruence (Figure 2C). For example, isolate 3671 had a γ lineage allele at
331 GRA7, but a δ lineage allele at BAG1. Recombination within a single chromosome VIIa was
332 also observed at linked markers (GRA7 and SAG4) for 18 strains (Figure 2D). Here, isolate
333 3387 had a γ lineage allele at GRA7, but a δ lineage allele at SAG4, whereas 3675 had a II
334 lineage allele at GRA7, but a γ lineage allele at SAG4. These results confirm that
335 recombination had occurred and support genetic hybridization as the most plausible
336 explanation for the origin of the 12 Type X haplotypes.
337
338 **Type X is an admixture between Type II and a novel genetic background by CGH-array**
339 **hybridization**
340 A subset of Type X isolates, 2 each from haplotypes A (3142, 3265), C (3026, 3045), F
341 (3503, 3429) and one each from D (3178) and H (3671) were hybridized against a
342 photolithographic microarray that possessed 1517 polymorphic Type I, II and III strain-
343 specific genotyping probes distributed genome-wide [36]. This was done to test whether the
344 MLST genetic markers accurately predicted the presence of large genome-wide haplotype
345 specific blocks, consistent with genetic hybridization. Each Type-specific SNP on the CGH
346 array is represented as a dot colored either red, green, or blue, respectively for a hybridizing
347 strain that possesses a Type I, II or III SNP at the probe position. Grey dots identified probes
348 that failed to hybridize, consistent with strains that do not possess a Type I, II or III specific
349 SNP at the probe position. Hybridization with DNA from a Type I (GT1), Type II (Me49), and
350 Type III (CTG) strain identified hybridization patterns consistent with genotype, indicating
351 that all genotype-specific probes were functioning as expected (Figure 3A). Hybridization
352 with the Type X isolates identified large, contiguous Type II haploblocks, as evidenced by
353 hybridization of all Type II-specific probes present on Chr III, VI, VIIb, and XII, for example.
354 However, in other portions of the genome, the SNP diversity pattern was novel. The
355 hybridization pattern in these regions either shared patch-work similarity with Type I (i.e.,
356 at Chr Ib, VI), or was highly divergent, with large contiguous blocks of SNP probes that failed
357 to hybridize (indicated by grey coloration), consistent with introgression of a non-Type I, II
358 or III genetic ancestry, rather than minor mutational drift (i.e., Chr IV, XI, right end of Chr VII,
359 XII, left end of Chr VIII).
360 The pattern of hybridizing SNPs was unique for each of the seven Type X isolates, but
361 it was only minimally different; either 3, 5, or 15 SNP differences were detected in pairwise
362 comparisons within haplotype A (3142, 3265), C (3026, 3045), and F (3503, 3429),
363 respectively (Figure 3A). At this resolution, it was not possible to distinguish between CGH
364 array hybridization efficiency and minor mutational drift. Indeed, the CGH arrays each had
365 approximately the same number of SNP differences (3-15) between haplotypes as they did
366 within each haplotype; this is more consistent with hybridization efficiency as the

367 explanation for hybridization differences. Further, this analysis established that the *T. gondii*
368 isolate 3671 is a novel genetic admixture, because it possessed a distinct Type II
369 hybridization pattern at Chr Ia, the left side of Chr Ib, VI, XI, and right side of Chr XII that
370 differed from all other Type X strains (Figure 3A).
371
372 **Type X is a recombinant clade at WGS resolution**
373 Due to the limited number of SNPs and differences in hybridization efficiency using the
374 CGH array approach, WGS was required to infer an accurate genetic history model for the
375 Type X strains. Using genome-wide polymorphism data, 568,592 variable SNP positions
376 were resolved after reference mapping the Type I, II, III, 16 SSO isolates (14 Type X, 2 Type
377 II), and three previously WGS sequenced HG12 isolates (WTD-1, RAY, ARI) against the
378 published Me49 genome. We next performed an unrooted Neighbor-Net analysis (Figure 3B)
379 that resolved the Type X strains into 15 distinct haplotypes at WGS resolution (Supplemental
380 Figure 1) and established that all Type X isolates, similar to Type I and III strains, shared
381 blocks of genome-wide ancestry with Type II, represented by the reticulated pattern of edge
382 blocks that depict recombination events between Type II and the different genetic
383 backgrounds within X, which were distinct from I and III. Our data did not support a clonal
384 lineage designation, as most Type X isolates appeared on separate branches (Figure 3B,
385 Inset). Only clonal complexes 1 and 4 (CC1, Type II; CC4, 3045, 3160, 4167) were supported
386 at WGS resolution, and 3 previously sequenced HG12 strains isolated from 2 people (ARI,
387 RAY) and a deer (WTD-1) formed well-supported clades with Type X isolates 4166 (WTD-1;
388 RAY) and 3168 (ARI), indicating that Type X has a broad host distribution that extends
389 beyond sea otters. Outside of the reticulated network of edge blocks, the branch length for
390 each Type X isolate was significantly less than that observed for Type I and III, synonymous
391 with a more recent origin, without sufficient time to accumulate private SNPs by mutational
392 drift. When murine virulence data for each genotype was mapped onto the Neighbor-Net
393 tree (see inset, Figure 3B), a clear partitioning of the different virulence phenotypes was
394 resolved along branches within the network, consistent with Type X isolates existing as
395 sister progeny, with only minor mutational drift detected at each supported branch.
396 To identify the size, genome distribution, and total number of Type II admixed
397 haploblocks introgressed into each Type X isolate, pairwise SNP diversity plots were
398 generated for all Type X isolates, as well as reference Type I and III strains that have been
399 previously shown to have recombined with Type II. The Type I GT1 strain possessed an Me49
400 Chr Ia and IV, and an Me49 admixture block at the left side of Chr VIIa, and right end of Chr
401 XI (Figure 4). As expected, the Type III VEG strain possessed many more Me49 admixture
402 blocks distributed genome-wide than GT1, comprising ~40% of its genome. Only Type X
403 haplotype H (3671) possessed haploblocks that were highly similar in sequence to Me49, on
404 Chr Ia, II, III, VI, VIII, IX, XI, and XII (Figure 4). In other regions, however, 3671 shared regions
405 clearly Me49-like, but that appeared to have diverged somewhat by mutational drift
406 (average 3-5 SNPs per 10kb block) on Chr II, or introgressed into Chr IV, V, VIIa, VIIb, VIII,
407 IX, and XII. Intermixed within the Type II regions of the 3671 genome were a limited number
408 of large haploblocks containing divergent SNP density synonymous with hybridization by a
409 strain possessing distinct γ or δ genetic ancestry (average of 50-100 SNPs per 10kb block).
410 When the pairwise SNP density analysis was expanded to different Type X haplotypes,
411 isolates within each haplotype possessed highly similar patchwork mosaics of Type II-like
412 or divergent (Type X) haploblocks that were specific to each haplotype. For example,

413 haplotype A isolates 3142 and 3168 SNP density plots were highly similar to each other, and
414 to haplotype C isolate 3045, but were readily distinguishable from isolates 4166 and 3503;
415 strains within haplotypes D and F, respectively (Figure 4). Specifically, isolate 3142 had a
416 Type X haploblock inheritance pattern at the right end of Chr V, and in the middle of Chr Ib,
417 VIIa, VIII, IX and XII, whereas 4166, which was indistinguishable from a previously
418 sequenced HG12 strain (RAY) recovered from a human patient, possessed either Type II or
419 3671 haploblocks in these regions (Figure 4). Although the haplotype F isolate 3503 was
420 highly similar in genomic organization to 3142, it possessed a Type II haploblock at the right
421 end of Chr V that readily distinguished it from haplotype A. The pairwise SNP analysis
422 established that most Type X haplotypes possess a genomic architecture that is strikingly
423 similar, but different at a limited number of admixture blocks. Coupled with the low allelic
424 diversity, the data support a genetic history model whereby Type X resembles a sexual clade
425 of recently-derived natural recombinants from a relatively limited number of crosses.
426
427 **PopNet analysis identifies only limited admixture blocks among Type X isolates**
428 While the Neighbor-Net analysis established that Type X exists as a recombinant clade of
429 strains, it failed to predict the precise number of genetic ancestries, or how they had admixed
430 positionally across the chromosomes. PopNet was used to paint chromosomes according to
431 their local inheritance patterns [37]. Included in the analysis were all sequenced Type X and
432 II strains, as well as reference Type I and III strains known to have admixed with Type II.
433 PopNet identified 4 statistically supported ancestries and showed that each genome was a
434 mosaic of these distinct ancestries, further supporting the admixture model.
435 Within the circle depicting the Type X clade, 5 distinct subgroupings were identified
436 based on the number and position of shared ancestral blocks; these were grouped together
437 based on line thickness (Figure 5A). These same groupings were supported both by Pairwise
438 SNP plots and Neighbor-Net analysis, but the PopNet analysis showed which of the 5
439 ancestries had introgressed positionally across the mosaic genomes. Clear recombination
440 blocks were readily resolved, and the genome architecture was remarkably similar between
441 the groupings. A custom script designed to identify only major crossover points between the
442 two parents (Type II and the mosaic ancestry of the γ/δ parent) identified either a limited
443 number of single and double recombination events, or the inheritance of whole
444 chromosomes of either Type II (Chr II) or γ/δ (Chr Ia, IV, XI) parental ancestry, consistent
445 with this group of strains representing related sister progeny (Figure 5B). Because murine
446 virulence plotted on the Neighbor-Net tree identified clear pathogenicity differences in mice
447 that clustered based on parasite genotype, and that the Type X strains resembled a natural
448 clade of recombinant progeny (akin to F_1) that possessed only a restricted number of
449 crossover points, a population-based QTL was performed to see if genes could be mapped
450 that contributed to murine virulence within the set of 18 natural isolates for which virulence
451 data existed (Figure 5C),
452
453 **Natural Population-based QTL identifies ROP33 (WNG-3) as a new murine Vir locus**
454 All Type X isolates recovered from sea otters resembled offspring from one (or a few
455 crosses) between a Type II strain, which is avirulent in mice, and unknown parent(s) that
456 are a mosaic of two distinct ancestries. Because these natural isolates possessed a range of
457 virulence phenotypes in laboratory-exposed mice (Figure 1C), a genome scan was performed

458 to determine the log-likelihood for association of discrete genome haploblocks with the
459 acute virulence phenotype. Four quantitative trait loci (QTL) peaks were identified with
460 logarithm of odds (LOD) scores 4.0 or greater on chromosomes V, VIIa, VIII, and X (Figure
461 6A). The average size of the genomic regions spanned by the QTLs were in the range of 100-
462 200kb, except for one on chromosome V, which was >700 kb (Figure 6B). To identify
463 candidate genes within the four peaks, the following inclusion criteria were assessed:
464 presence of a signal peptide and/or transmembrane domain, gene expression and
465 polymorphism differences, as well as every gene's CRISPR genome-wide mutagenesis score
466 for essentiality [38] (Supplemental Table 2). *ROP33* on chromosome VIIa stood out as the
467 best candidate gene to target for reverse genetics as it was abundantly expressed during
468 acute infection, it was predicted to be a functional serine-threonine protein kinase, it was
469 highly polymorphic, and is part of a family of divergent WNG (with-no-Gly-loop) kinases that
470 regulate parasite tubular membrane biogenesis [33]. Further, one allele of *ROP33* was
471 strongly correlated with acute virulence in mice (p=0.00031; fishers two-sided exact test)
472 (Figure 6C).
473 To determine whether *ROP33* was a novel murine virulence gene, the *ROP33* locus was
474 disrupted by targeted deletion using CRISPR-Cas9 facilitated double crossover homologous
475 recombination in the RHΔ*ku80*Δ*rop18*Δ*hxgprt* strain [39]. This strain is virulent in mice
476 (LD_{100}=500 tachyzoites) and was engineered to accept targeted replacement of the *rop33*
477 gene using an HXGPRT gene flanked by 30bp of homology just outside of the *rop33* promoter
478 and 3'UTR region. Following selection in mycophenolic acid (MPA) and xanthine (to select
479 for the *HXGPRT* gene), the population was screened for disruption of the *rop33* gene by PCR.
480 Mice were next infected with either the parent RHΔ*ku80*Δ*rop18*Δ*hxgprt* strain or the Rop33^{-}
481 mutant to assess virulence. Groups of 5 outbred CD1 mice were injected intraperitoneally
482 with 500 tachyzoites and the results shown are for one of two replicates. All mice infected
483 with the parent RH line succumbed to infection within 20 days (Figure 6D). In contrast,
484 targeted deletion of the *rop33* gene was protective, with most (9/10) mice surviving acute
485 infection. Our results suggest that ROP33 is an acute virulence gene for *T. gondii*.
486 Importantly, the lack of virulence for parasite strains with deletion of the *rop33* gene was not
487 the result of a failure of the mutant parasite to proliferate *in vivo*, as no difference in parasite
488 load was detected through acute infection by bioluminescence imaging (Figure 6E). All
489 surviving mice were seropositive for *T. gondii*, indicating that they had been productively
490 infected. These data suggest that ROP33 is a new virulence factor for murine infection and
491 that this mouse-virulence gene was identified from wild-derived *T. gondii* isolates that had
492 undergone a population genetic cross in a natural setting.
493
494 **Discussion**
495 We investigated the emergence of a suspected clonal lineage of *T. gondii* (Type X; also
496 referred to as HG12) from isolates recovered longitudinally from a single marine host
497 (southern sea otters) in California over seven years (1998-2004). Our goal was to determine
498 the genetic basis for the emergence of this unique *T. gondii* lineage in a federally listed,
499 threatened species. Although Type X had previously been identified as the 4th clonal lineage
500 in North American wildlife, our work established that Type X is not a clonal lineage, but
501 rather a recombinant clade of strains that resemble F_1 progeny from at least one natural
502 cross. DNA sequence analysis using diverse linked and unlinked markers across the nuclear
503 and organellar genomes of Type X isolates identified Type X to be a composite of Type II, and

504 a mosaic of two distinct ancestries, referred to as γ and δ, that had recombined to produce a
505 highly invasive clade of strains causing both subclinical infection and mortality in a
506 threatened marine mammal.

507 Our data suggest that Type X was derived from one or a limited number of natural
508 crosses between two highly related parental strains. One sea otter genotype (Type X
509 haplotype A) was widely distributed and was found to have expanded to cause most
510 subclinical infections in sampled sea otters, but was highly virulent to laboratory-exposed
511 mice. Our isolates from a naturally-infected wild animal population support a model
512 whereby *T. gondii*'s sexual life cycle is facilitating the evolution and expansion of cryptically
513 virulent strains that can cause significant morbidity and mortality in a species-specific
514 manner. For generalist parasites like *T. gondii* that have broad host ranges, natural selection
515 among intermediate hosts appears to maximize transmission and may establish how
516 virulent strains can be maintained cryptically in nature. The expansion of a mouse virulent
517 clone into a new ecological niche, such as nearshore marine mammals of the Eastern Pacific
518 coastline, demonstrates how *T. gondii* is leveraging its intermediate host range to selectively
519 partition parasite genetic diversity and epidemic disease potential.

520 In prior studies, unknown strains having a distinct ancestry, referred to as α and β,
521 were found to have crossed with Type II to create the Type I and Type III clonal strains,
522 respectively [11]. The frequency and pattern of recombined blocks inherited within the Type
523 X strains is parsimonious with previously described models for the genetic history of Types
524 I and III in which an unidentified ancestor (respectively α and β) sexually recombined with
525 an ancestral Type II to create new lineages (Figure 5B) [11, 40]. Prior studies have suggested
526 that Type X is a product of genetic hybridization between a Type II lineage and an unknown
527 γ lineage [25, 27, 28, 32, 41]. In the current study, we have further refined this perspective
528 and concluded that Type X is a mosaic of a cross between Type II strains and two distinct
529 γ and δ ancestries. The γ/δ lineage has likely recombined at least once with Type II to create
530 the Type X recombinant clade of strains. Currently, no single isolate has been found which
531 could be defined as either γ or δ, similar to the α and β lines thought to have admixed with
532 Type II to produce the clonal lines I and III [11, 40].

533 Previous work on Type X circulating in wildlife samples using a limited set of
534 genotyping markers, including sea otters, identified Type X as the 4th clonal lineage in North
535 America [27, 28]. However, this designation was based on the discovery of genetically
536 distinct alleles at only a few loci, including GRA6, B1 and SAG1, which was the original basis
537 for distinguishing the Type X lineage as distinct from Type II, and that it had undergone a
538 hybridization event with a novel genotype [25]. It is now well established that Type X strains
539 commonly infect wildlife across North America [14, 26-30, 32, 35]. This study examined *T.*
540 *gondii* strains isolated longitudinally across a 7 year period and a 680 km expanse along the
541 California coast from stranded southern sea otters. Our sample set was comprised of otters
542 with *T. gondii* infections that ranged from subclinical to fatal.

543 Because previous work had classified Type X as clonal, detection of multiple disease
544 states among infected sea otters was unexpected [27, 28, 32, 35]. To ascertain whether
545 parasite genotype was influencing the observed disease spectrum, genotyping studies were
546 carried out using an expanded set of markers to more definitively characterize the
547 population genetic structure of Type X isolates. All genotyping markers used in this study
548 were sequenced to increase resolution rather than evaluated strictly for their PCR-RFLP

549 genotype, as was standard for many prior studies. While the PCR-DNA-Seq markers used
550 herein only surveyed a small part of the genome, they established that strains genotyped as
551 Type X via GRA6 and SAG1 alleles were in fact comprised of at least 12 distinct haplotypes
552 that could not be classified as minor variants based on relatively few SNP differences, as
553 concluded previously [26]. Furthermore, at any given locus, only a Type II allele or one or
554 another of two distinct alleles was identified, indicating limited allelic diversity and a total
555 lack of private SNPs. Hence, each of the 12 haplotypes possessed one of just three allelic types
556 at any one locus that had independently segregated across all examined markers. This result
557 is parsimonious with a recombinant clade of strains that reflect genetic hybrids from a
558 limited, but distinct set of ancestries.
559 Our results were further confirmed both by CGH array analyses and whole genome
560 sequencing. The previous misclassification as a clonal population appears to be the result of
561 the low resolution genotyping analyses performed, and the placement of the markers in
562 predominantly Type II regions of the genome [14, 28, 42]. For this reason, future studies
563 should use WGS to discriminate between haplogroups within a population and determine
564 the true genetic ancestry of each haplogroup. *Toxoplasma gondii* population genetics would
565 also greatly benefit from examination of an increased number of isolates at whole genome
566 sequencing resolution. Hence, WGS should be expanded to include a greater diversity of
567 strains, and multiple isolates from within each canonical clonal lineage.
568 The Type I and III clonal lineages are thought to be derived from a limited number of
569 sexual crosses, and all strains within these clonotypes share large haploblocks of Type II-like
570 sequence [11, 41-43]. This finding also holds true for the Type X lineage. At all MLST loci
571 surveyed, all Type X isolates possessed at least one marker that was Type II, and the
572 introgression of large haploblocks of Type II ancestry across each genome was confirmed in
573 the 19 strains that were resolved at WGS resolution. In regions that did not clade with Type
574 II, two different allelic types were identified. We concluded that these represented distinct
575 ancestries that we referred to as γ and δ. This designation was supported by the inherent
576 reticulation of the clade, seen in the NeighborNet tree (Figure 2B). Predominantly short
577 branch lengths radiating from a reticulated network with multiple strains on a single branch
578 were resolved, rather than a star-like phylogeny with multiple alleles present at each major
579 branch (the result of private SNPs that accumulated through genetic drift). In fact, the lack
580 of genetic drift between these loci supported genetic hybridization as the most parsimonious
581 explanation for the relationship between the Type X haplotypes.
582 Sexual replication with genetic recombination is known to occur in *T. gondii* strains in
583 South America at high frequency [40, 42, 44]. Recent studies on the population genetic
584 structure of *T. gondii* have also established that genetic hybridization, at whole genome
585 resolution, is extant for most sequenced strains that represent the breadth of genetic
586 diversity within *T. gondii* [15, 37]. Evidence of sexual recombination across the population,
587 and evidence of sexual replication within the Type X clade shown here, may indicate that
588 sexual recombination is occurring more frequently than previously suspected among *T.*
589 *gondii* strains circulating within North America.
590 No barriers appear to exist, or have been described, to limit sexual recombination of *T.*
591 *gondii* from occurring in a laboratory setting, although there is incomplete understanding of
592 the genetic factors regulating sexual replication in felid hosts [7, 43, 45-47]. It is not clear
593 why sexual recombination is reported less commonly in North American wildlife, when
594 compared to South America, although it is possible that self-mating within dominant

595 populations in North America is masking the detection of genetic outcrossing [12, 41, 48].
596 Among closely related isolates, unisexual mating (defined as intra-lineage crosses between
597 similar strains that possess distinct genotypes) cannot be resolved using current genotyping
598 methods that rely on low-resolution analyses, and thus cannot readily distinguish asexual
599 expansion from unisexual mating [12].

600 *Toxoplasma gondii* has been shown to utilize its sexual cycle to expand its biological
601 potential and alter its pathogenesis [7, 45, 47]. Sexual recombination, by the ability to
602 reshuffle parental alleles into new combinations, can produce progeny with diverse
603 biological potential [7]. Our work identified a single *T. gondii* genotype (Type X haplotype A)
604 that was presumably derived from a recent genetic cross and naturally selected in southern
605 sea otters. Although most haplotype A-infected sea otters had mild infections, this genotype
606 was highly pathogenic to outbred laboratory mice, with all mice dying in 10-15 days after
607 administering as few as 50 tachyzoites. In contrast, three Type X haplotype F isolates were
608 highly pathogenic to sea otters but significantly less so to outbred laboratory mice
609 (Supplemental Figure 1). Our data support a virulence shift model for the expansion and
610 propagation of *T. gondii* in nature, whereby the parasite utilizes its sexual cycle to generate
611 a diverse spectrum of new genotypes that possess altered biological potential that can be
612 naturally selected across *T. gondii*'s vast host range to optimize parasite transmission, and
613 colonize new niches. Hence, natural selection among intermediate hosts allows *T. gondii* to
614 maintain highly pathogenic strains cryptically; these strains can cause serious disease in
615 some animal hosts, but not others.

616 This type of selection has been observed previously in laboratory mice that express
617 variable IRG (Immunity Related GTPase) gene arrays. IRGs are host proteins primarily
618 responsible for combatting *T. gondii* lysis of murine cells. The *T. gondii* genome encodes a
619 suite of highly polymorphic rhoptry kinase genes (ROPKs) that function to inactivate host
620 IRGs [49-51]. While laboratory mice are highly clonal, wild mice and their subsequent IRGs
621 are more diverse, as are the ROPKs expressed by *T. gondii* strains that are capable of infecting
622 wild mice [17, 52]. As a result, different *T. gondii* genotypes are naturally selected in wild
623 mice based on the combination of host IRGs versus ROPK alleles expressed. Hence, wild CIM
624 mice do not succumb to *T. gondii* Type I infections, whereas laboratory mice do.

625 Similarly, TLR 11/12 is a primary rodent innate immune response sensor (otherwise
626 referred to as PAMPs) that detects *T. gondii* infection. Not all intermediate hosts share a
627 functional combination of TLR11/12; *T. gondii* strains that are selected for mouse infection
628 must bypass TLR11/12 recognition, while this is not a barrier to infection of human cells [52,
629 53]. As a result, intermediate hosts are capable of naturally selecting *T. gondii* strain
630 genotypes that establish chronic, transmissible infections in a host-specific and parasite
631 strain-dependent manner. To optimize its biological potential, the parasite must find a
632 balance between virulence, fitness, and infectious transmissibility across a wide host range.
633 It is this capacity to maintain cryptically virulent strains that may contribute to *T. gondii's*
634 global distribution and success in nature; it has the ability to cause disease outbreaks,
635 expand its host range into new ecological niches, or alter its pathogenicity in both a parasite
636 strain-specific and host-specific manner to maximize transmission.

637 For other protozoan parasites, host partitioning is usually synonymous with speciation.
638 For example, *Plasmodium* spp. often partition by the mosquito host species they co-evolved
639 with to maximize parasite transmission [54-58]. Likewise, *Sarcocystis* spp. largely maintain
640 separate parasite species for each intermediate-definitive host species combination to

641 maintain its life cycle [12, 59]. In contrast, *T. gondii* forms transmissible cysts in virtually all
642 warm-blooded vertebrates, and these cysts are infectious for its definitive felid host as well
643 as diverse intermediate hosts. The difference is that across the genetic diversity of *T. gondii*,
644 specific parasite genotypes are being selectively expanded within different intermediate
645 hosts, based primarily on parasite genotype and the suite of polymorphic effector proteins
646 encoded by each parasite strain. This allows *T. gondii* to maintain cryptically virulent strains
647 across a broad intermediate host range, with intermediate hosts playing a central role in the
648 natural selection, expansion, and maintenance of virulent strains across the host range of
649 this generalist parasite. In effect, infected hosts can act as reservoirs for the pathogenic or
650 epidemic potential of the species.
651 Our study showed that one sub-type of *T. gondii* which had expanded in most sea otters
652 (where it caused primarily subclinical, chronic infections) was uniformly lethal to outbred
653 laboratory mice. This is similar to another sub-type of *T. gondii* that express predominantly
654 Type I alleles and chronically infect wild birds which is highly pathogenic in exposed
655 laboratory mice [60]. Additionally, while Type II isolates commonly infect domestic livestock
656 in North America, Type X is more common in sylvatic hosts, prompting the hypothesis that
657 separate cycles exist within the *T. gondii* population that overlap solely within the feline
658 definitive host [10, 29, 61].
659 Finally, only a limited number of crossovers were detected among strains that were WGS
660 sequenced within the recombinant clade of Type X haplotypes. Because the pedigree of one
661 of the parents was known, we concluded that the isolates resembled F_1 progeny from a
662 natural cross, which prompted us to perform a population-based QTL analysis on an
663 unmanipulated, natural population of genetic hybrids. Taking advantage of a genome-wide,
664 high resolution SNP map we had generated for all sequenced haplotypes, our analysis
665 identified multiple punctate QTL peaks containing a limited number of candidate loci
666 associated with differences in mouse virulence for reverse genetic follow-up. The serine-
667 threonine protein kinase ROP33 stood out as the best candidate to influence pathogenicity;
668 it was previously identified as an active protein kinase that is both abundantly expressed
669 and highly polymorphic. Further, ROP33 is a divergent WNG kinase (WNG-3) that is related
670 to ROP35 (WNG-1); a critical regulator of tubular membrane biogenesis, the formation of the
671 parasite's intravesicular network (or IVN), and the phosphorylation of dense granule
672 proteins associated with IVN biogenesis [33]. In fact, dense granule proteins GRA2 and GRA6
673 are required for IVN biogenesis, and IVN-deficient parasites grow normally *in vitro*, but are
674 attenuated in mouse virulence assays [62, 63]. Related ROP proteins, including ROP 5, 16,
675 17, and 18 are known to hijack host immune signaling pathways to alter *T. gondii* virulence
676 during rodent infection.
677 However, all Type X isolates investigated in our study, whether mouse virulent or
678 avirulent, only expressed avirulent allele combinations of the known ROP 5/16/18 virulence
679 factors. We chose to knock-out the gene in a Ku80 deficient strain of *T. gondii* that was both
680 mouse virulent, and deficient in ROP18 because no change in mouse virulence was reported
681 when ROP33 was deleted in a wild-type RH strain background [64]. In addition, previous
682 genetic mapping studies failed to identify the QTL for this locus, even though it is
683 polymorphic between Type I, II and III strains for which genetic crosses have been
684 performed. It is likely that the ROP5 and ROP18 virulence factors were dominant, and ROP33
685 is analogous to ROP17; another virulence factor that was only identified after the virulence
686 enhancing capacity of ROP18 was removed [39].

687 Our results show that parasites deficient in ROP33 in the highly permissive
688 RHΔku80Δ*rop18* parent were avirulent, whereas an infectious dose of 500 tachyzoites of the
689 RHΔku80Δ*rop18* parent genotype was uniformly virulent in mice. Specifically how ROP33
690 contributes to murine virulence, what dense granule proteins it phosphorylates, the integrity
691 of the IVN and what host immune signaling pathways are modified are being actively
692 investigated. Future work will dissect the host or parasite factors that ROP33 targets to
693 reduce or influence parasite transmission and pathogenicity. Finally, our study establishes
694 that it is possible to use *T. gondii* isolates derived from a naturally-occurring population
695 genetic cross to identify genetic loci associated with a specific quantitative phenotype.
696
697 **Materials and Methods**
698
699 **Parasite culture**
700 Fifty-three previously published *T. gondii* strains isolated from brain and/or other
701 tissue samples from stranded southern sea otters were provided by Dr. Patricia Conrad [25,
702 26]. Aseptically-collected tissue for parasite isolation was obtained during gross necropsy of
703 sea otters at the Marine Wildlife Veterinary Care and Research Center in Santa Cruz, CA.
704 Parasite isolation in tissue culture was performed at the University of California, Davis
705 School of Veterinary Medicine, as described [25]. The primary and any contributing causes
706 of death (COD), sequelae, and incidental findings were determined for each sea otter based
707 on gross necropsy and histopathology, as described [25, 26, 31, 65]. The coastal location for
708 each stranded sea otter, as well as the associated *T. gondii* isolate, was noted to the nearest
709 0.5 km along the central California coast as ATOS ("as the otter swims") numbers. Isolates
710 were named sequentially based on the sea otter number and stranding year. Due to multiple
711 encounters with the same otter over its lifetime, sea otter case number 3142 was later
712 corrected to 2922, but both numbers represent the same animal; this is indicated in
713 Supplementary Figure 1. Parasites were maintained in vitro in human foreskin fibroblast
714 (HFF) monolayers as described [66].
715
716 **DNA extraction and genetic typing markers**
717 Cultivated parasites were syringe lysed using a 27-gauge needle and filtered through
718 a 3.0 micron polycarbonate filter to remove cellular debris. DNA was extracted from cell
719 pellets using the Qiagen DNeasy Blood and Tissue kit (Qiagen). All 53 isolates were typed
720 using 5 previously described PCR-RFLPs, and one DNA sequencing marker [7, 25, 67-69].
721 BSR4, BAG1, and ROP1 were PCR amplified and typed based on known RFLP identity. GRA6
722 and SAG3 were typed according to previously identified representative SNPs based on
723 Sanger sequence data by the National Institute of Allergy and Infectious Disease's Rocky
724 Mountain Laboratory (NIAID RML).
725 Alleles observed via sequencing were designated as canonical I, II, or III. When
726 sequences differed from canonical alleles, previously described methods of characterization
727 were used [29]. Briefly, when genetic variation differed from references by two mutations
728 or more, the allele was classified as a novel allele, whereas only one mutation was labeled as
729 a drifted allele from the closest reference sequence.
730 Twenty-one strains representing the 8 unique genotypes identified by the 5 markers
731 applied herein were then selected for additional characterization. These 21 strains were PCR
732 amplified, sequenced, and genotyped using 20 markers: 18 at both linked and unlinked

genomic loci, encompassing 13 of the 14 chromosomes, and 2 loci on organellar genomes (apicoplast and mitochondria), representing 15,430 bp with 335 SNPs (~0.024% of the genome). Sequences were examined and nucleotides were verified using SeqMan Pro alignment software (Lasergene). Sequences for reference strains (ME49, GT1, and VEG) were downloaded from ToxoDB [70].

Generation of the *ROP33* knockout strain in *RHΔku80Δhxgprt* parasites

Deletion of the *ROP33* gene was generated using the Type I parasite RH that was rendered deficient in the expression of *KU80* and the drug selectable marker *HXGPRT*. Briefly, the CRISPR/Cas9 targeting plasmid pSAG1:CAS9,U6:sgUPRT (received from Prof. L. David Sibley, Department of Molecular Microbiology, Washington University School of Medicine) was modified with a guide RNA (GTCGGACGCGAAACTCGCTT) to target the 5' region of the *ROP33* gene (sgROP33) using Q5 mutagenesis (New England Biolabs, MA). Then a CRISPR/Cas9 replacement construct was created using Gibson assembly (New England Biolabs) to stitch together a 1kb flanking region of the 5' UTR region of ROP33 (TGGT1_chrVIIa, 3921773 to 3922773 bp) with the selectable marker HXGPRT and a 1kb flanking region of the 3'UTR region of ROP33 (TGGT1_chrVIIa, 3926189 to 3927189 bp) to replace the *ROP33* gene using the selectable drug cassette. To delete the *ROP33* gene, a total of 50 µg of the sgROP33 and replacement construct (5:1 ratio) were co-transfected into a ROP18 deficient strain of RH (RH *Δku80ΔhxgprtΔrop18*), which was cultured in human foreskin fibroblasts (HFF) cells and maintained in Dulbecco's modified Eagle's medium (DMEM) supplemented with 10% fetal bovine serum, 2 mM glutamine and 25 µg / ml gentamicin. After transfection, parasites were selected for stable integration of the targeting construct using mycophenolic acid (12.5 mg / mL in MeOH; MPA) / xanthine (20 mg / mL in 1M KOH; XAN) as described [71]. After 15 days, the resistant population was cloned by limiting dilution and single clones were screened by PCR for targeted deletion of the *ROP33* gene.

Mouse virulence assay

To determine the virulence of the sea otter *T. gondii* isolates in a mouse model, groups of five or more, 6-8 week-old, female CD1 outbred mice were intraperitoneally injected with 50 *T. gondii* tachyzoites resuspended in 500 µl of PBS that had been expanded in HFF cells. Mice were weighed daily to measure infection-induced cachexia, and mouse survival was assayed over 42 days [7]. At 14 days, mice were bled, and serum was extracted to test for seroconversion via indirect fluorescent antibody test (IFAT) against ME49 tachyzoites [72]. Strain virulence was classified as follows: avirulent strains killed no seropositive mice within 42 days of infection, intermediate virulent strains killed some but not all seropositive mice within 42 days post-infection, and virulent strains killed all seropositive mice. To assess the contribution of ROP33 to mouse virulence, groups of five, 6-8 week old female outbred CD1 mice were injected intraperitoneally with 500 tachyzoites of either the parent RHΔ*ku80*Δ*rop18*Δ*hxgprt* strain, or the *Rop33*$^{-}$ mutant; infectivity and virulence were assessed as above.

Phylogenetic Tree and DNA Marker Analysis

The default settings of Clustal X were used to align DNA sequences for all markers individually and as a concatenated set [73]. MSF files of aligned marker sequences were

779 imported into Molecular Evolutionary Genetic Analysis (MEGA) Version 7 to create a
780 maximum likelihood tree using Tamura-Nei model distance analysis with uniform rates of
781 substitution across all sites, and 1000 bootstrap support for all branch points [74].
782 Consensus trees were rooted on ME49, as Type II is an inherent parent in all strains analyzed.
783 All scales were set at 0.001 nucleotide difference unit. Distinct parental lineages with
784 bootstrap support over 60% were indicated on each tree to distinguish II alleles from novel
785 γ and δ alleles. These novel alleles were indicated in purple and orange respectively for the
786 17 MLST loci (Supplementary Table 2). The Nexus file of the concatenated marker alignment
787 was imported into SplitsTree 4 Version 4.13.1 where NetworkNet analysis was run using
788 default settings [75].
789
790 **eBURST Clonal Complex Analysis**
791 Alleles determined from the 17 nuclear encoded markers (excluding ROP1 due to its
792 classification as a microsatellite marker) were given numerical designations to create a
793 multilocus sequence-typing scheme for the eBURST program [76]. Default settings were
794 used to evaluate strain-specific alleles. Individual strains were displayed as dots with unique
795 colors: Type I, II, III, and X strains were represented by red, green, blue, and purple dots
796 respectively, and dot size reflected the number of strains assessed within each genotype.
797 Strains sharing 16 of the 17 nuclear encoded markers were designated as clonal complexes,
798 represented by interconnecting lines in the diagram.
799
800 **Genomic hybridization to Affymetrix arrays**
801 Genomic DNA was sheared and biotin labeled before hybridizing to a custom *T. gondii*
802 Affymetrix microarray as previously published [36]. High-fidelity SNPs were characterized
803 via a custom R script to identify SNPs belonging to each of the three reference strains (I, II,
804 and III). Three reference strains (GT1, ME49, and CTG) were shown to demonstrate ideal
805 hybridization within canonical lineages. Sea otter Type X DNA isolate hybridizations were
806 shown below the reference strains.
807
808 **Whole-Genome Sequence Analysis of Type X Recombination**
809 DNA was isolated from 16 southern sea otter *T. gondii* isolates with optimal tissue
810 culture properties, plus 3 representative Type X strains (ARI, RAY, and WTD1), for a total of
811 19 *T. gondii* strains. Three micrograms of *T. gondii* DNA isolated from each of the 19 strains
812 was sent to NIAID RML for whole-genome sequencing using Illumina HiSeq technology. Fastq
813 reads were reference mapped to the *T. gondii* ME49 assemblage Version 8.2 [70] using BWA
814 0.7.5a to align the reads to the reference genome and GATK 3.7 in coordination with Picard
815 1.131, and following best practices *T. gondii* for quality control of mapped reads [77].
816 Following mapping, the gVCF method of GATK was used to combine SNP calls using
817 stand_call_conf of 30.0, nct of 10, and ploidy of 1 (for haploid genomes) to call 568,592 single
818 nucleotide polymorphism positions across the whole genomes of these strains [77]. The
819 derived VCF formatted SNP file was curated using GATK and VCFTools to produce a tabular
820 file containing only biallelic SNPs with no large insertions or deletions [81]. A custom script
821 was then utilized to convert this SNP file into a fasta file of strain polymorphic positions
822 across the Type X and reference genomes. These SNP fasta files were run in SplitsTree4 using
823 default parameters for BioNJ with 1000 bootstrap support to create a NeighborNet tree [70].

824 Interconnected reticulation between strains was indicative of recombination between
825 strains, whereas mitotic drift was visualized by divergent branching.
826
827 **SNP Density Fingerprint Analysis of Recombinant Progeny**
828 The same tabular, biallelic SNP file used in the NeighborNet analysis was modified
829 using a custom R script based on location mapping to isolate strain-specific polymorphic
830 locations from the tabular VCF. Further R scripts grouped these SNPs into 100 kb windows,
831 which were mapped across the genomes of the sea otter-origin and representative Type X *T.*
832 *gondii* strains to highlight differences from the reference genome (ME49) [44, 82]. The larger
833 the number of SNPs in a particular window, the more divergent the strain was from the ME49
834 reference. Distinct haploblocks where genomic recombination had occurred were apparent
835 in areas where haploblock diversity significantly varied from the surrounding regions on the
836 same chromosome.
837
838 **PopNet Characterization of Strain Interrelatedness**
839 The tabular, biallelic SNP file created from WGS of Type X and used to derive the SNP
840 density plots and NeighborNet tree was uploaded into PopNet using default parameters to
841 assess the diversity and interrelatedness of strains [38]. Cytoscape was used to visualize the
842 recombination and Markov clustering outputs. Genomes were displayed in circularized
843 format with chromosomes concatenated into a circular genome display. The background of
844 each isolate was painted to match with the group that shared the most common ancestry
845 over the entire genome. Chromosome painting was done in 10 kb increments and the
846 sequence haploblock was painted based on its shared ancestry. For instance, a Type X isolate
847 haploblock that was most closely related to the ancestral Type II strain was painted green to
848 indicate its inheritance. Strains that were more closely related had thicker connecting lines
849 between the circles for each of the *T. gondii* isolates.
850
851 **Virulence Gene Identification by QTL**
852 To identify novel virulence alleles, the tabular, biallelic SNP file was utilized to run a
853 quantitative trait locus (QTL) analysis on the Type X and Type II *T. gondii* isolates that were
854 sequenced to WGS resolution [83]. SNP calls were down-selected by a custom java script to
855 include one SNP every 5 kb. This allows the QTL software to analyze the breadth of the
856 WGS data in QTL, which was built to handle marker typing data without the depth inherent
857 in WGS data. Custom scripts coded the SNPs into reference (ME49) versus alternative
858 (Type X's γ/δ lineage which substituted as the secondary parent) alleles. This down-
859 selected marker dataset was combined with previously determined low-dose inoculum
860 murine virulence data for the same strains. This combined data was then inputted into J/qtl
861 and a one QTL genome scan was run using the default settings for the EM algorithm
862 (maximum likelihood) with 1000 permutations to identify genomic locations that were
863 significantly associated with mouse death due to Type X infection [84].
864 The QTL calculations identified four genomic regions with a LOD score of greater than
865 4.0 that were significantly associated with an enhanced risk of mouse death. Within these
866 genomic regions, 450 genes were predicted based on ToxoDB documentation. These
867 potential genes were down-selected based on presence of a signal peptide and/or
868 transmembrane domain, gene expression, polymorphism, and genome-wide CRISPR score

869 for essentiality to identify 32 virulence candidate genes within the Type X strains. Of these,
870 ROP33 was selected for further interrogation based on its high LOD score and similarity to
871 previously identified virulence effector proteins.
872
873 **Funding statement:**
874 This work was supported in part by the Intramural Research Program of the National
875 Institute of Allergy and Infectious Diseases (NIAID) at the National Institutes of Health and
876 by the National Science Foundation, Ecology of Infectious Diseases Grant 052576. Sea otter
877 disease investigations at the California Department of Fish and Wildlife were supported in
878 part by citizens of California through the California Sea Otter Fund.
879
880 **Ethics statements:**
881 The animal study protocol LPD 22E was reviewed and approved by the Animal Care and Use
882 Committee of the Intramural Research Program of the National Institute of Allergy and
883 Infectious Diseases, National Institutes of Health. No human studies or identifiable human
884 data are presented in this study. All datasets generated for this study are available upon
885 request to the corresponding author.
886
887 **Acknowledgements**
888 We thank Patricia Conrad for critically reading and providing comments on the manuscript.
889 We thank Andrea Packham and Ann Melli for their assistance in culturing and isolation of
890 the *T. gondii* isolates, and Javi Zhang for his help with PopNet analysis. We thank Michael
891 Murray of the Monterey Bay Aquarium and Frances Gulland of the Marine Mammal Center
892 for the submission of additional sea otter cases that yielded *T. gondii* isolates that were not
893 previously characterized. We also thank all volunteers and staff at the California
894 Department of Fish and Wildlife, the Monterey Bay Aquarium, the Marine Mammal Center,
895 and the United States Geological Survey for their efforts to recover stranded sea otters that
896 facilitated the isolation of *T. gondii* strains utilized in this paper. This study used the Office
897 of Cyber Infrastructure and Computational Biology (OCICB) High Performance Computing
898 (HPC) cluster at the National Institute of Allergy and Infectious Diseases (NIAID), Bethesda,
899 MD.
900
901
902 **References**
903 1. Vijaykrishna D, Smith GJ, Pybus OG, Zhu H, Bhatt S, Poon LL, et al. Long-term
904 evolution and transmission dynamics of swine influenza A virus. Nature.
905 2011;473(7348):519-22. doi: 10.1038/nature10004. PubMed PMID: 21614079.
906 2. Bellanger X, Payot S, Leblond-Bourget N, Guedon G. Conjugative and mobilizable
907 genomic islands in bacteria: evolution and diversity. FEMS Microbiol Rev. 2014;38(4):720-
908 60. doi: 10.1111/1574-6976.12058. PubMed PMID: 24372381.
909 3. Schneider G, Dobrindt U, Middendorf B, Hochhut B, Szijarto V, Emody L, et al.
910 Mobilisation and remobilisation of a large archetypal pathogenicity island of uropathogenic
911 Escherichia coli in vitro support the role of conjugation for horizontal transfer of genomic
912 islands. BMC Microbiol. 2011;11:210. doi: 10.1186/1471-2180-11-210. PubMed PMID:
913 21943043; PubMed Central PMCID: PMC3202238.

914 4. Wardal E, Markowska K, Zabicka D, Wroblewska M, Giemza M, Mik E, et al.
915 Molecular analysis of vanA outbreak of Enterococcus faecium in two Warsaw hospitals: the
916 importance of mobile genetic elements. Biomed Res Int. 2014;2014:575367. doi:
917 10.1155/2014/575367. PubMed PMID: 25003118; PubMed Central PMCID: PMC4070583.
918 5. English ED, Adomako-Ankomah Y, Boyle JP. Secreted effectors in Toxoplasma gondii
919 and related species: determinants of host range and pathogenesis? Parasite Immunol.
920 2015;37(3):127-40. doi: 10.1111/pim.12166. PubMed PMID: 25655311.
921 6. Fraser JA, Giles SS, Wenink EC, Geunes-Boyer SG, Wright JR, Diezmann S, et al. Same-
922 sex mating and the origin of the Vancouver Island Cryptococcus gattii outbreak. Nature.
923 2005;437(7063):1360-4. Epub 2005/10/14. doi: 10.1038/nature04220. PubMed PMID:
924 16222245.
925 7. Grigg ME, Bonnefoy S, Hehl AB, Suzuki Y, Boothroyd JC. Success and virulence in
926 toxoplasma as the result of sexual recombination between two distinct ancestries. Science.
927 2001;294(5540):161-5. doi: DOI 10.1126/science.1061888. PubMed PMID:
928 WOS:000171448800052.
929 8. Boothroyd JC, Grigg ME. Population biology of Toxoplasma gondii and its relevance
930 to human infection: do different strains cause different disease? Curr Opin Microbiol. 5.
931 England2002. p. 438-42.
932 9. Boyer K, Hill D, Mui E, Wroblewski K, Karrison T, Dubey JP, et al. Unrecognized
933 ingestion of Toxoplasma gondii oocysts leads to congenital toxoplasmosis and causes
934 epidemics in North America. Clin Infect Dis. 2011;53(11):1081-9. Epub 2011/10/25. doi:
935 10.1093/cid/cir667. PubMed PMID: 22021924; PubMed Central PMCID: PMCPMC3246875.
936 10. Behnke MS, Khan A, Wootton JC, Dubey JP, Tang K, Sibley LD. Virulence differences
937 in Toxoplasma mediated by amplification of a family of polymorphic pseudokinases. Proc
938 Natl Acad Sci U S A. 2011;108(23):9631-6. doi: 10.1073/pnas.1015338108. PubMed PMID:
939 21586633; PubMed Central PMCID: PMC3111276.
940 11. Boyle JP, Rajasekar B, Saeij JP, Ajioka JW, Berriman M, Paulsen I, et al. Just one cross
941 appears capable of dramatically altering the population biology of a eukaryotic pathogen
942 like Toxoplasma gondii. Proc Natl Acad Sci U S A. 2006;103(27):10514-9. doi:
943 10.1073/pnas.0510319103. PubMed PMID: 16801557; PubMed Central PMCID:
944 PMC1502489.
945 12. Wendte JM, Miller MA, Lambourn DM, Magargal SL, Jessup DA, Grigg ME. Self-mating
946 in the definitive host potentiates clonal outbreaks of the apicomplexan parasites
947 Sarcocystis neurona and Toxoplasma gondii. PLoS Genet. 2010;6(12):e1001261. doi:
948 10.1371/journal.pgen.1001261. PubMed PMID: 21203443; PubMed Central PMCID:
949 PMC3009688.
950 13. Boothroyd JC. Expansion of host range as a driving force in the evolution of
951 Toxoplasma. Memorias Do Instituto Oswaldo Cruz. 2009;104(2):179-84. PubMed PMID:
952 WOS:000267051500009.
953 14. Howe DK, Sibley LD. Toxoplasma gondii comprises three clonal lineages: correlation
954 of parasite genotype with human disease. J Infect Dis. 1995;172(6):1561-6. PubMed PMID:
955 7594717.
956 15. Lorenzi H, Khan A, Behnke MS, Namasivayam S, Swapna LS, Hadjithomas M, et al.
957 Local admixture of amplified and diversified secreted pathogenesis determinants shapes
958 mosaic Toxoplasma gondii genomes. Nat Commun. 2016;7:10147. doi:

959 10.1038/ncomms10147. PubMed PMID: 26738725; PubMed Central PMCID:
960 PMCPMC4729833.
961 16. Sibley LD, Boothroyd JC. Virulent strains of Toxoplasma gondii comprise a single
962 clonal lineage. Nature. 1992;359(6390):82-5. doi: 10.1038/359082a0. PubMed PMID:
963 1355855.
964 17. Lilue J, Muller UB, Steinfeldt T, Howard JC. Reciprocal virulence and resistance
965 polymorphism in the relationship between Toxoplasma gondii and the house mouse. Elife.
966 2013;2:e01298. doi: 10.7554/eLife.01298. PubMed PMID: 24175088; PubMed Central
967 PMCID: PMC3810784.
968 18. Steinfeldt T, Konen-Waisman S, Tong L, Pawlowski N, Lamkemeyer T, Sibley LD, et
969 al. Phosphorylation of mouse immunity-related GTPase (IRG) resistance proteins is an
970 evasion strategy for virulent Toxoplasma gondii. PLoS Biol. 2010;8(12):e1000576. Epub
971 2011/01/05. doi: 10.1371/journal.pbio.1000576. PubMed PMID: 21203588; PubMed
972 Central PMCID: PMCPMC3006384.
973 19. Cavailles P, Sergent V, Bisanz C, Papapietro O, Colacios C, Mas M, et al. The rat Toxo1
974 locus directs toxoplasmosis outcome and controls parasite proliferation and spreading by
975 macrophage-dependent mechanisms. Proc Natl Acad Sci U S A. 2006;103(3):744-9. Epub
976 2006/01/13. doi: 10.1073/pnas.0506643103. PubMed PMID: 16407112; PubMed Central
977 PMCID: PMCPMC1334643.
978 20. Cirelli KM, Gorfu G, Hassan MA, Printz M, Crown D, Leppla SH, et al. Inflammasome
979 sensor NLRP1 controls rat macrophage susceptibility to Toxoplasma gondii. PLoS Pathog.
980 2014;10(3):e1003927. Epub 2014/03/15. doi: 10.1371/journal.ppat.1003927. PubMed
981 PMID: 24626226; PubMed Central PMCID: PMCPMC3953412.
982 21. Ewald SE, Chavarria-Smith J, Boothroyd JC. NLRP1 is an inflammasome sensor for
983 Toxoplasma gondii. Infect Immun. 2014;82(1):460-8. Epub 2013/11/13. doi:
984 10.1128/IAI.01170-13. PubMed PMID: 24218483; PubMed Central PMCID:
985 PMCPMC3911858.
986 22. Gorfu G, Cirelli KM, Melo MB, Mayer-Barber K, Crown D, Koller BH, et al. Dual role
987 for inflammasome sensors NLRP1 and NLRP3 in murine resistance to Toxoplasma gondii.
988 MBio. 2014;5(1). Epub 2014/02/20. doi: 10.1128/mBio.01117-13. PubMed PMID:
989 24549849; PubMed Central PMCID: PMCPMC3944820.
990 23. Dubey JP, Shen SK, Kwok OC, Frenkel JK. Infection and immunity with the RH strain
991 of Toxoplasma gondii in rats and mice. J Parasitol. 1999;85(4):657-62. PubMed PMID:
992 10461945.
993 24. Conrad PA, Miller MA, Kreuder C, James ER, Mazet J, Dabritz H, et al. Transmission of
994 Toxoplasma: clues from the study of sea otters as sentinels of Toxoplasma gondii flow into
995 the marine environment. Int J Parasitol. 2005;35(11-12):1155-68. Epub 2005/09/15. doi:
996 10.1016/j.ijpara.2005.07.002. PubMed PMID: 16157341.
997 25. Miller MA, Grigg ME, Kreuder C, James ER, Melli AC, Crosbie PR, et al. An unusual
998 genotype of Toxoplasma gondii is common in California sea otters (Enhydra lutris nereis)
999 and is a cause of mortality. Int J Parasitol. 2004;34(3):275-84. doi:
1000 10.1016/j.ijpara.2003.12.008. PubMed PMID: 15003489.
1001 26. Shapiro K, VanWormer E, Packham A, Dodd E, Conrad PA, Miller M. Type X strains of
1002 Toxoplasma gondii are virulent for southern sea otters (Enhydra lutris nereis) and present
1003 in felids from nearby watersheds. Proc Biol Sci. 2019;286(1909):20191334. Epub

1004 2019/08/23. doi: 10.1098/rspb.2019.1334. PubMed PMID: 31431162; PubMed Central
1005 PMCID: PMCPMC6732395.
1006 27. Khan A, Dubey JP, Su C, Ajioka JW, Rosenthal BM, Sibley LD. Genetic analyses of
1007 atypical Toxoplasma gondii strains reveal a fourth clonal lineage in North America. Int J
1008 Parasitol. 2011;41(6):645-55. doi: 10.1016/j.ijpara.2011.01.005. PubMed PMID:
1009 21320505; PubMed Central PMCID: PMC3081397.
1010 28. Dubey JP, Velmurugan GV, Rajendran C, Yabsley MJ, Thomas NJ, Beckmen KB, et al.
1011 Genetic characterisation of Toxoplasma gondii in wildlife from North America revealed
1012 widespread and high prevalence of the fourth clonal type. Int J Parasitol.
1013 2011;41(11):1139-47. doi: 10.1016/j.ijpara.2011.06.005. PubMed PMID: 21802422.
1014 29. VanWormer E, Miller MA, Conrad PA, Grigg ME, Rejmanek D, Carpenter TE, et al.
1015 Using molecular epidemiology to track Toxoplasma gondii from terrestrial carnivores to
1016 marine hosts: implications for public health and conservation. PLoS Negl Trop Dis.
1017 2014;8(5):e2852. doi: 10.1371/journal.pntd.0002852. PubMed PMID: 24874796; PubMed
1018 Central PMCID: PMC4038486.
1019 30. Gibson AK, Raverty S, Lambourn DM, Huggins J, Magargal SL, Grigg ME.
1020 Polyparasitism is associated with increased disease severity in Toxoplasma gondii-infected
1021 marine sentinel species. PLoS Negl Trop Dis. 2011;5(5):e1142. doi:
1022 10.1371/journal.pntd.0001142. PubMed PMID: 21629726; PubMed Central PMCID:
1023 PMC3101184.
1024 31. Kreuder C, Miller MA, Jessup DA, Lowenstine LJ, Harris MD, Ames JA, et al. Patterns
1025 of mortality in southern sea otters (Enhydra lutris nereis) from 1998-2001. J Wildl Dis.
1026 2003;39(3):495-509. doi: 10.7589/0090-3558-39.3.495. PubMed PMID: 14567210.
1027 32. Sundar N, Cole RA, Thomas NJ, Majumdar D, Dubey JP, Su C. Genetic diversity among
1028 sea otter isolates of Toxoplasma gondii. Vet Parasitol. 2008;151(2-4):125-32. doi:
1029 10.1016/j.vetpar.2007.11.012. PubMed PMID: 18155841.
1030 33. Beraki T, Hu X, Broncel M, Young JC, O'Shaughnessy WJ, Borek D, et al. Divergent
1031 kinase regulates membrane ultrastructure of the Toxoplasma parasitophorous vacuole.
1032 Proc Natl Acad Sci U S A. 2019;116(13):6361-70. Epub 2019/03/10. doi:
1033 10.1073/pnas.1816161116. PubMed PMID: 30850550; PubMed Central PMCID:
1034 PMCPMC6442604.
1035 34. Miller MA, Miller WA, Conrad PA, James ER, Melli AC, Leutenegger CM, et al. Type X
1036 Toxoplasma gondii in a wild mussel and terrestrial carnivores from coastal California: new
1037 linkages between terrestrial mammals, runoff and toxoplasmosis of sea otters. Int J
1038 Parasitol. 2008;38(11):1319-28. doi: 10.1016/j.ijpara.2008.02.005. PubMed PMID:
1039 18452923.
1040 35. Su C, Khan A, Zhou P, Majumdar D, Ajzenberg D, Darde ML, et al. Globally diverse
1041 Toxoplasma gondii isolates comprise six major clades originating from a small number of
1042 distinct ancestral lineages. Proc Natl Acad Sci U S A. 2012;109(15):5844-9. doi:
1043 10.1073/pnas.1203190109. PubMed PMID: 22431627; PubMed Central PMCID:
1044 PMCPMC3326454.
1045 36. Khan A, Miller N, Roos DS, Dubey JP, Ajzenberg D, Darde ML, et al. A monomorphic
1046 haplotype of chromosome Ia is associated with widespread success in clonal and nonclonal
1047 populations of Toxoplasma gondii. MBio. 2011;2(6):e00228-11. doi: 10.1128/mBio.00228-
1048 11. PubMed PMID: 22068979; PubMed Central PMCID: PMC3215432.

1049 37. Zhang J, Khan A, Kennard A, Grigg ME, Parkinson J. PopNet: A Markov Clustering
1050 Approach to Study Population Genetic Structure. Mol Biol Evol. 2017;34(7):1799-811. Epub
1051 2017/04/07. doi: 10.1093/molbev/msx110. PubMed PMID: 28383661; PubMed Central
1052 PMCID: PMCPMC5850731.
1053 38. Sidik SM, Huet D, Ganesan SM, Huynh MH, Wang T, Nasamu AS, et al. A Genome-wide
1054 CRISPR Screen in Toxoplasma Identifies Essential Apicomplexan Genes. Cell.
1055 2016;166(6):1423-35 e12. Epub 2016/09/07. doi: 10.1016/j.cell.2016.08.019. PubMed
1056 PMID: 27594426; PubMed Central PMCID: PMCPMC5017925.
1057 39. Etheridge RD, Alaganan A, Tang K, Lou HJ, Turk BE, Sibley LD. The Toxoplasma
1058 pseudokinase ROP5 forms complexes with ROP18 and ROP17 kinases that synergize to
1059 control acute virulence in mice. Cell Host Microbe. 2014;15(5):537-50. Epub 2014/05/17.
1060 doi: 10.1016/j.chom.2014.04.002. PubMed PMID: 24832449; PubMed Central PMCID:
1061 PMCPMC4086214.
1062 40. Khan A, Fux B, Su C, Dubey JP, Darde ML, Ajioka JW, et al. Recent transcontinental
1063 sweep of Toxoplasma gondii driven by a single monomorphic chromosome. Proc Natl Acad
1064 Sci U S A. 2007;104(37):14872-7. Epub 2007/09/07. doi: 10.1073/pnas.0702356104.
1065 PubMed PMID: 17804804; PubMed Central PMCID: PMCPMC1965483.
1066 41. Grigg ME, Sundar N. Sexual recombination punctuated by outbreaks and clonal
1067 expansions predicts Toxoplasma gondii population genetics. Int J Parasitol.
1068 2009;39(8):925-33. doi: 10.1016/j.ijpara.2009.02.005. PubMed PMID: 19217909; PubMed
1069 Central PMCID: PMC2713429.
1070 42. Minot S, Melo MB, Li F, Lu D, Niedelman W, Levine SS, et al. Admixture and
1071 recombination among Toxoplasma gondii lineages explain global genome diversity.
1072 Proceedings of the National Academy of Sciences of the United States of America.
1073 2012;109(33):13458-63. doi: DOI 10.1073/pnas.1117047109. PubMed PMID:
1074 WOS:000307807000067; PubMed Central PMCID: PMCPMC3421188.
1075 43. Khan A, Shaik JS, Behnke M, Wang QL, Dubey JP, Lorenzi HA, et al. NextGen
1076 sequencing reveals short double crossovers contribute disproportionately to genetic
1077 diversity in Toxoplasma gondii. Bmc Genomics. 2014;15. doi: Artn 1168
1078 10.1186/1471-2164-15-1168. PubMed PMID: WOS:000349049000003.
1079 44. Rajendran C, Su C, Dubey JP. Molecular genotyping of Toxoplasma gondii from
1080 Central and South America revealed high diversity within and between populations. Infect
1081 Genet Evol. 2012;12(2):359-68. Epub 2012/01/10. doi: 10.1016/j.meegid.2011.12.010.
1082 PubMed PMID: 22226702.
1083 45. Saeij JP, Boyle JP, Coller S, Taylor S, Sibley LD, Brooke-Powell ET, et al. Polymorphic
1084 secreted kinases are key virulence factors in toxoplasmosis. Science.
1085 2006;314(5806):1780-3. doi: 10.1126/science.1133690. PubMed PMID: 17170306;
1086 PubMed Central PMCID: PMC2646183.
1087 46. Saeij JP, Coller S, Boyle JP, Jerome ME, White MW, Boothroyd JC. Toxoplasma co-opts
1088 host gene expression by injection of a polymorphic kinase homologue. Nature.
1089 2007;445(7125):324-7. doi: 10.1038/nature05395. PubMed PMID: 17183270; PubMed
1090 Central PMCID: PMC2637441.
1091 47. Taylor S, Barragan A, Su C, Fux B, Fentress SJ, Tang K, et al. A secreted serine-
1092 threonine kinase determines virulence in the eukaryotic pathogen Toxoplasma gondii.
1093 Science. 2006;314(5806):1776-80. doi: 10.1126/science.1133643. PubMed PMID:
1094 17170305.

1095 48. Ferguson D. Toxoplasma gondii and sex: essential or optional extra? Trends
1096 Parasitol. 2002;18(8):351. Epub 2002/10/16. PubMed PMID: 12377284.
1097 49. Fleckenstein MC, Reese ML, Konen-Waisman S, Boothroyd JC, Howard JC, Steinfeldt
1098 T. A Toxoplasma gondii pseudokinase inhibits host IRG resistance proteins. PLoS Biol.
1099 2012;10(7):e1001358. doi: 10.1371/journal.pbio.1001358. PubMed PMID: 22802726;
1100 PubMed Central PMCID: PMC3393671.
1101 50. Hunn JP, Feng CG, Sher A, Howard JC. The immunity-related GTPases in mammals: a
1102 fast-evolving cell-autonomous resistance system against intracellular pathogens. Mamm
1103 Genome. 2011;22(1-2):43-54. doi: 10.1007/s00335-010-9293-3. PubMed PMID:
1104 21052678; PubMed Central PMCID: PMC3438224.
1105 51. Yamamoto M, Okuyama M, Ma JS, Kimura T, Kamiyama N, Saiga H, et al. A cluster of
1106 interferon-gamma-inducible p65 GTPases plays a critical role in host defense against
1107 Toxoplasma gondii. Immunity. 2012;37(2):302-13. doi: 10.1016/j.immuni.2012.06.009.
1108 PubMed PMID: 22795875.
1109 52. Gazzinelli RT, Mendonca-Neto R, Lilue J, Howard J, Sher A. Innate Resistance against
1110 Toxoplasma gondii: An Evolutionary Tale of Mice, Cats, and Men. Cell Host Microbe.
1111 2014;15(2):132-8. Epub 2014/02/18. doi: 10.1016/j.chom.2014.01.004. PubMed PMID:
1112 24528860.
1113 53. Koblansky AA, Jankovic D, Oh H, Hieny S, Sungnak W, Mathur R, et al. Recognition of
1114 profilin by Toll-like receptor 12 is critical for host resistance to Toxoplasma gondii.
1115 Immunity. 2013;38(1):119-30. doi: 10.1016/j.immuni.2012.09.016. PubMed PMID:
1116 23246311; PubMed Central PMCID: PMC3601573.
1117 54. Mackinnon MJ, Read AF. Virulence in malaria: an evolutionary viewpoint. Philos
1118 Trans R Soc Lond B Biol Sci. 2004;359(1446):965-86. doi: 10.1098/rstb.2003.1414.
1119 PubMed PMID: 15306410; PubMed Central PMCID: PMC1693375.
1120 55. Ariey F, Witkowski B, Amaratunga C, Beghain J, Langlois AC, Khim N, et al. A
1121 molecular marker of artemisinin-resistant Plasmodium falciparum malaria. Nature.
1122 2014;505(7481):50-5. Epub 2013/12/20. doi: 10.1038/nature12876. PubMed PMID:
1123 24352242.
1124 56. Bopp SE, Manary MJ, Bright AT, Johnston GL, Dharia NV, Luna FL, et al. Mitotic
1125 evolution of Plasmodium falciparum shows a stable core genome but recombination in
1126 antigen families. PLoS Genet. 2013;9(2):e1003293. doi: 10.1371/journal.pgen.1003293.
1127 PubMed PMID: 23408914; PubMed Central PMCID: PMC3567157.
1128 57. Miotto O, Almagro-Garcia J, Manske M, Macinnis B, Campino S, Rockett KA, et al.
1129 Multiple populations of artemisinin-resistant Plasmodium falciparum in Cambodia. Nat
1130 Genet. 2013;45(6):648-55. Epub 2013/04/30. doi: 10.1038/ng.2624. PubMed PMID:
1131 23624527; PubMed Central PMCID: PMC3807790.
1132 58. Arisue N, Hashimoto T. Phylogeny and evolution of apicoplasts and apicomplexan
1133 parasites. Parasitol Int. 2014. doi: 10.1016/j.parint.2014.10.005. PubMed PMID: 25451217.
1134 59. Barbosa L, Johnson CK, Lambourn DM, Gibson AK, Haman KH, Huggins JL, et al. A
1135 novel Sarcocystis neurona genotype XIII is associated with severe encephalitis in an
1136 unexpectedly broad range of marine mammals from the northeastern Pacific Ocean. Int J
1137 Parasitol. 2015. doi: 10.1016/j.ijpara.2015.02.013. PubMed PMID: 25997588.
1138 60. Dubey JP, Graham DH, da Silva DS, Lehmann T, Bahia-Oliveira LM. Toxoplasma
1139 gondii isolates of free-ranging chickens from Rio de Janeiro, Brazil: mouse mortality,

1140 genotype, and oocyst shedding by cats. J Parasitol. 2003;89(4):851-3. Epub 2003/10/10.
1141 doi: 10.1645/GE-60R. PubMed PMID: 14533703.
1142 61. Wendte JM, Gibson AK, Grigg ME. Population genetics of Toxoplasma gondii: new
1143 perspectives from parasite genotypes in wildlife. Vet Parasitol. 2011;182(1):96-111. doi:
1144 10.1016/j.vetpar.2011.07.018. PubMed PMID: 21824730; PubMed Central PMCID:
1145 PMC3430134.
1146 62. Labruyere E, Lingnau M, Mercier C, Sibley LD. Differential membrane targeting of
1147 the secretory proteins GRA4 and GRA6 within the parasitophorous vacuole formed by
1148 Toxoplasma gondii. Mol Biochem Parasitol. 1999;102(2):311-24. Epub 1999/09/25. doi:
1149 10.1016/s0166-6851(99)00092-4. PubMed PMID: 10498186.
1150 63. Mercier C, Howe DK, Mordue D, Lingnau M, Sibley LD. Targeted disruption of the
1151 GRA2 locus in Toxoplasma gondii decreases acute virulence in mice. Infect Immun.
1152 1998;66(9):4176-82. Epub 1998/08/26. PubMed PMID: 9712765; PubMed Central PMCID:
1153 PMCPMC108503.
1154 64. Wang JL, Li TT, Elsheikha HM, Chen K, Zhu WN, Yue DM, et al. Functional
1155 Characterization of Rhoptry Kinome in the Virulent Toxoplasma gondii RH Strain. Front
1156 Microbiol. 2017;8:84. Epub 2017/02/09. doi: 10.3389/fmicb.2017.00084. PubMed PMID:
1157 28174572; PubMed Central PMCID: PMCPMC5258691.
1158 65. Miller MA, Gardner IA, Packham A, Mazet JK, Hanni KD, Jessup D, et al. Evaluation of
1159 an Indirect Fluorescent Antibody Test (Ifat) for Demonstration of Antibodies to
1160 Toxoplasma Gondii in the Sea Otter (Enhydra Lutris). Journal of Parasitology.
1161 2002;88(3):594-9. doi: 10.1645/0022-3395(2002)088[0594:eoaifa]2.0.co;2.
1162 66. Pszenny V, Angel SO, Duschak VG, Paulino M, Ledesma B, Yabo MI, et al. Molecular
1163 cloning, sequencing and expression of a serine proteinase inhibitor gene from Toxoplasma
1164 gondii. Mol Biochem Parasitol. 2000;107(2):241-9. PubMed PMID: 10779600.
1165 67. Su C, Zhang X, Dubey JP. Genotyping of Toxoplasma gondii by multilocus PCR-RFLP
1166 markers: a high resolution and simple method for identification of parasites. Int J Parasitol.
1167 2006;36(7):841-8. doi: 10.1016/j.ijpara.2006.03.003. PubMed PMID: 16643922.
1168 68. Fazaeli A, Carter PE, Darde ML, Pennington TH. Molecular typing of Toxoplasma
1169 gondii strains by GRA6 gene sequence analysis. Int J Parasitol. 2000;30(5):637-42. PubMed
1170 PMID: 10779578.
1171 69. Howe DK, Sibley LD. Toxoplasma gondii: analysis of different laboratory stocks of
1172 the RH strain reveals genetic heterogeneity. Exp Parasitol. 1994;78(2):242-5. doi:
1173 10.1006/expr.1994.1024. PubMed PMID: 7907030.
1174 70. Gajria B, Bahl A, Brestelli J, Dommer J, Fischer S, Gao X, et al. ToxoDB: an integrated
1175 Toxoplasma gondii database resource. Nucleic Acids Res. 2008;36(Database issue):D553-6.
1176 doi: 10.1093/nar/gkm981. PubMed PMID: 18003657; PubMed Central PMCID:
1177 PMC2238934.
1178 71. Donald RG, Carter D, Ullman B, Roos DS. Insertional tagging, cloning, and expression
1179 of the Toxoplasma gondii hypoxanthine-xanthine-guanine phosphoribosyltransferase gene.
1180 Use as a selectable marker for stable transformation. J Biol Chem. 1996;271(24):14010-9.
1181 Epub 1996/06/14. doi: 10.1074/jbc.271.24.14010. PubMed PMID: 8662859.
1182 72. Fletcher S. Indirect Fluorescent Antibody Technique in the Serology of Toxoplasma
1183 Gondii. J Clin Pathol. 1965;18:193-9. Epub 1965/03/01. PubMed PMID: 14276154; PubMed
1184 Central PMCID: PMC472865.

1185 73. Larkin MA, Blackshields G, Brown NP, Chenna R, McGettigan PA, McWilliam H, et al.
1186 Clustal W and Clustal X version 2.0. Bioinformatics. 2007;23(21):2947-8. doi:
1187 10.1093/bioinformatics/btm404. PubMed PMID: 17846036.
1188 74. Tamura K, Stecher G, Peterson D, Filipski A, Kumar S. MEGA6: Molecular
1189 Evolutionary Genetics Analysis version 6.0. Mol Biol Evol. 2013;30(12):2725-9. doi:
1190 10.1093/molbev/mst197. PubMed PMID: 24132122; PubMed Central PMCID:
1191 PMC3840312.
1192 75. Huson DH, Bryant D. Application of phylogenetic networks in evolutionary studies.
1193 Mol Biol Evol. 2006;23(2):254-67. doi: 10.1093/molbev/msj030. PubMed PMID:
1194 16221896.
1195 76. Feil EJ, Li BC, Aanensen DM, Hanage WP, Spratt BG. eBURST: Inferring Patterns of
1196 Evolutionary Descent among Clusters of Related Bacterial Genotypes from Multilocus
1197 Sequence Typing Data. Journal of Bacteriology. 2004;186(5):1518-30. doi:
1198 10.1128/jb.186.5.1518-1530.2004.
1199 77. Van der Auwera GA, Carneiro MO, Hartl C, Poplin R, Del Angel G, Levy-Moonshine A,
1200 et al. From FastQ data to high confidence variant calls: the Genome Analysis Toolkit best
1201 practices pipeline. Curr Protoc Bioinformatics. 2013;11(1110):11 0 1- 0 33. doi:
1202 10.1002/0471250953.bi1110s43. PubMed PMID: 25431634; PubMed Central PMCID:
1203 PMC4243306.
1204
1205 **Competing interests**
1206 The authors declare no competing financial interests.
1207
1208 **Figure Legends**
1209 **<u>Figure 1</u>: Parasite diversity and mouse virulence within the *Toxoplasma gondii* Type X**
1210 **clade infecting southern sea otters (*Enhydra lutris nereis*)**
1211 A) Fifty-three *T. gondii* isolates from southern sea otters necropsied 1998-2004 were
1212 genotyped using 5 unlinked markers, resulting in the identification of 9 distinct *T. gondii*
1213 genotypes. Type I, II, and III alleles are represented by red, green, and blue bars, respectively.
1214 Sea otters were infected with *T. gondii* strains that possessed either non-archetypal alleles
1215 (purple or orange bars) or a Type II allele (green bars) at the loci examined. For each distinct
1216 genotype, the number of *T. gondii* infected sea otters (#SO) and its percentage of total
1217 infections (%SO) is shown. Each distinct genotype was comprised of the following *T. gondii*
1218 isolates which corresponds to the sequential stranding number of each stranded sea otter: **A**
1219 (3097, 3142, 3168, 3265, 3483, 3488, 3520, 3637, 3659, 3744, 3786, 3821, 3865, 3947, 3950,
1220 4003, 4045, 4071, 4151), **B** (3458, 3523, 3728, 3897), **C** (3026, 3045, 3077, 3160, 4167), **D**
1221 (3133, 3178, 3183, 3451, 4166), **E** (3819), **F** (3387, 3429, 3503), **G** (3675), **H** (3671), **II**
1222 (2987, 2994, 3005, 3009, 3087, 3131, 3208, 3396, 3521, 3576, 3587, 3636, 3739, 4181).
1223 B) Distribution of isolates recovered from *T. gondii*-infected sea otters by genotype and
1224 stranding year (1998-2003): Type II (green) versus Type X haplotype (various shades of
1225 purple). Although the sample size was small, Type II infections appeared to cluster
1226 temporally, whereas Type X haplotype A infections (dark purple bars), isolated from sea
1227 otters with predominantly subclinical or incidental infections, appeared to increase in the
1228 final year of the study.
1229 C) Cohorts of CD1 mice were infected with 50 tachyzoites each intraperitoneally with
1230 various *T. gondii* genotypes isolated from southern sea otters. Each mouse cohort was

1231 infected with one of 18 isolates representing all singletons (**E, G, H**), and at least two
1232 isolates each from the remaining 6 distinct genotypes (**II, A, B, C, D, F**). Mouse
1233 seroconversion and survival was monitored for 30 days. At least two independent infection
1234 experiments were performed using 5 mice for each isolate; results shown are only for mice
1235 that seroconverted and/or died acutely during infection. Strains are grouped and colored
1236 based on their genotype and virulence in mice. **Red**; mouse virulent, **Blue**; intermediate
1237 mouse virulent (some mice survived acute infection); **Green**; mouse avirulent (all mice
1238 survived acute infection). The number of mice infected by each genotype (as indicated by
1239 acute death and/or seropositivity) and their relative virulence is indicated at right.
1240 D) eBURST analysis to determine linkage disequilibrium across 17 nuclear-encoded
1241 linked and unlinked markers identified 4 clonal complexes and 3 unique Type X genotypes
1242 among 21 isolates selected from the 9 distinct clades in Figure 1A. Isolate colors represent
1243 the lineage Type from A: red (Type I), green (Type II), blue (Type III), and purple (Type X;
1244 all haplotypes (A-H)). Dot size is proportional to the number of isolates with that genotype;
1245 larger dots are multi-isolate genotypes. Clonal complexes (CC) are indicated by lines
1246 connecting isolates and are highlighted with ovals corresponding to their allelic identity (X-
1247 purple, II-green)
1248
1249 **Figure 2**: **Phylogenetic analyses support designation of Type X *Toxoplasma gondii***
1250 **isolates recovered from southern sea otters as a recombinant clade of related strains**
1251 Maximum likelihood trees of sequenced markers are depicted. Allele designations were
1252 dependent on a bootstrap support greater than 60%. Isolates are colored based on their
1253 genotype from Figure 1A (I: red, II: green, III: blue, X: purple). A) Mitochondrial marker, CO1.
1254 B) Nuclear genome marker BSR4 on Chromosome IV. At BSR4, all Type X strains possessed
1255 a single allele, referred to as γ that was readily distinguished from Type I, II and III alleles C)
1256 Comparison of two unlinked nuclear-encoded markers GRA7 and BAG1. At both markers,
1257 Type X strains possessed one of two distinct alleles, referred to as γ or δ. Isolates possessing
1258 δ alleles at both markers were highlighted in purple, those that possessed Type II alleles at
1259 both markers were highlighted in green. Isolates that were recombinant and possessed a γ
1260 allele at GRA7 but a δ allele at BAG1 were highlighted in pink, and conversely, a δ allele at
1261 GRA7 and a γ allele at BAG1 were highlighted in orange. D) Comparison of linked genomic
1262 markers GRA7 and SAG4. Genetic recombination is highlighted within this chromosome.
1263 Isolates that are linked and have Type II lineage alleles at both markers are highlighted in
1264 green. Isolates that show recombination between the γ/δ lineage alleles and the Type II
1265 lineage alleles are highlighted in pink and orange depending on recombination
1266 directionality.
1267
1268 **Figure 3**: **Genome-wide SNP typing of Type X *Toxoplasma gondii* isolates recovered**
1269 **from southern sea otters displays haploblock recombination across the genome**
1270 A) CGH-array hybridization of Type X strains against Type I, II and III lineage-specific probes
1271 identified 8 distinct Type II and non-Type II hybridization patterns across the 8 Type X
1272 strains examined. SNPs are represented by a dot in one of three rows indicating where the
1273 isolate has hybridized to the microarray with a hybridization characteristic of lineage Type
1274 I (red), II (green), or III (blue). Grey indicates no hybridization at this location. Chromosomes
1275 are represented as alternating grey and white bars.

1276 B) Linkage disequilibrium and network reticulation demonstrates the existence of recombination
1277 across the Type X genome. A NeighborNet tree based on whole genome sequence identified
1278 568,592 SNP variant positions across the 19 Type X strains reference mapped to ME49. Type I
1279 (red), II (green), III (blue), and X (purple) strains were annotated in the box beside the group based
1280 on their previous MLST designation. Two clusters of Type X strains were identified. Strains within
1281 the inset were colored based on their murine virulence: virulent (red), intermediate virulent (blue),
1282 avirulent (green), not assayed in mice (black).
1283
1284 **<u>Figure 4</u>: SNP density plots for *Toxoplasma gondii* isolates recovered from southern**
1285 **sea otters identify distinct and different recombination crossover points between the**
1286 **Type II and γ/δ lineage among examined Type X strains**
1287 WGS reads for all strains were mapped to the ME49 reference genome. Each row represents
1288 the SNPs of one strain mapped in a sliding 10 kb window across the genome, separated into
1289 chromosomes columns. Vertical bars across the row represent the number of SNPs, the
1290 height of the bar (from y-axis 0-200 bp) represents the amount of divergence from the ME49
1291 genome. Type X strains were grouped based on their MLST designation.
1292
1293 **<u>Figure 5</u>: Whole genome sequencing establishes *Toxoplasma gondii* Type X isolates**
1294 **recovered from southern sea otters as a recombinant clade of related strains**
1295 A) PopNet analysis for all strains sequenced at WGS resolution. The genome of each strain is
1296 represented by a circle of concatenated chromosomes starting at the top with Chromosome
1297 Ia and rotating clockwise to Chromosome XII. All strains were clustered into four distinct
1298 color groups based on their degree of shared ancestry (Type II-green, Type X-pink, Type I-
1299 cyan, Type III-blue) and each isolate has an inner circle that is arrayed in color-group
1300 haploblocks based on shared ancestry. Line thickness between strains indicates their
1301 interrelatedness, boldest lines indicate 90-100% of the genome is in linkage disequilibrium,
1302 as shown for strains 4167, 3819, 3045 and 3160.
1303 B) Genetic model showing cross-over recombination points for isolate 3142. Type II ancestry
1304 is shown in green whereas the mosaic of γ/δ ancestry is shown in black.
1305 C) 21 WGS isolates are shown with their group designation for the 5 loci MLST (Figure 1A),
1306 eBURST clonal complex identity (Figure 1D), 17 loci MLST (Supplemental Table 1), and
1307 murine virulence phenotype (Figure 1C).
1308
1309 **<u>Figure 6:</u> Population level QTL analysis identifies multiple chromosomal locations**
1310 **associated with acute murine virulence**
1311 A) WGS data from Type X strains was down-selected to one SNP every 5 kb and analyzed
1312 using standard QTL methods with 1000 bootstrap support. LOD scores are shown across the
1313 chromosomes for these strains based on genetic association with acute murine virulence as
1314 shown in Supplemental Table 2.
1315 B) Significantly associated peaks from the QTL were identified based on clusters of SNP
1316 peaks. The LOD scores for the tallest portion of the associated genomic region are listed.
1317 C) Distance-based Neighbor-joining ROP33 tree. Alignment of *ROP33* DNA sequences were
1318 used to construct a phylogenetic tree representing the majority of ROP33 alleles encoded
1319 within the species *Toxoplasma gondii.* Mouse virulence for each isolate is depicted by a color-
1320 code, per Figure 1C. **Red**, mouse virulent, **Blue**, intermediate mouse virulent (some CD-1

1321 mice survived acute infection); **Green**, mouse avirulent (all CD-1 mice survived acute
1322 infection). Inoculum size was 50 tachyzoites injected intraperitoneally in CD-1 outbred mice.
1323 D) Type I RH parasites deficient in ROP18 and ROP33 are less virulent than Type I RH
1324 parasites deficient in ROP18 alone, indicating that ROP33 is a virulence locus in *Toxoplasma.*
1325 CD-1 mice were infected intraperitoneally with 500 tachyzoites of the RH*Δrop18* or
1326 RH*Δrop18Δrop33* DKO, only the results for seropositive mice are shown. Data are combined
1327 from two independent experiments, each with five mice per group.
1328 E) Bioluminescent detection of parasite burden *in vivo* at 9 days post-infection of CD-1 mice
1329 with 50 tachyzoites injected intraperitoneally. A representative image with photon output
1330 in photons/second/cm2/surface radiance (*sr*) is shown.
1331
1332 **<u>Supplemental Figure 1</u>: Stranding location, necropsy date, sex, *Toxoplasma* IgG titer**
1333 **(IFAT), and *Sarcocystis neurona* co-infection status for *Toxoplasma gondii* isolates**
1334 **recovered from southern sea otters (1998-2004).**
1335 A) Coastal California stranding locations for all *Toxoplasma gondii* isolates recovered from
1336 southern sea otters (1998-2004). Each stranding location is represented by a red dot.
1337 B) *Toxoplasma gondii* isolates included in this study. Isolates in yellow were genotyped
1338 previously using PCR-RFLP analyses at 4 loci (*B1, SAG1, SAG2, SAG3*), and isolates 3131, 3133,
1339 3160, 3265 were DNA sequenced at the *GRA6 locus* [25]. WGS analysis further resolved the
1340 21 isolates into 15 distinct Type X genotypes (X1-X15) and two Type II strains. ATOS
1341 numbers and stranding locations identify the location of each stranded Sea otter. Isolates
1342 were grouped together based on their 5 locus DNA sequence genotype and then by their
1343 ATOS number. "Tg" indicates *Toxoplasma gondii,* "Sn" indicates co-infection with *Sarcocystis*
1344 *neurona*.
1345
1346 **<u>Supplemental Table 1</u>: Expanded sequencing marker genotyping of *Toxoplasma gondii***
1347 **Type X isolates recovered from southern sea otters reveals chromosomal segregation**
1348 **and recombination within chromosomes**
1349 Twenty-one isolates were characterized at 17 nuclear markers (ROP1 was excluded as it is
1350 a microsatellite marker, and prone to elevated mutation rates) clade into 12 distinct Type X
1351 genotypes (X1-X12). Isolate numbers in red were sequenced at whole-genome (WGS)
1352 resolution. Types I, II, III, γ and δ lineage alleles, as determined by phylogenetic comparisons,
1353 are colored red, green, blue, purple, and orange, respectively. Shades of colors represent
1354 genetic drift below the 60% bootstrap delineation from the canonical allele. White
1355 represents uninformative or incomplete DNA sequencing results.
1356
1357 **<u>Supplemental Table 2</u>: Potential virulence candidate genes derived from the QTL**
1358 **analysis**
1359 Chromosome peaks with LOD scores over 3 as shown in Figure 3B were interrogated via
1360 ToxoDB to select genes in these regions which have predicted signal sequences (Signal) and
1361 transmembrane (TM) domains in *Toxoplasma.* Genes are listed with gene ID, genomic
1362 location, and predicted protein function.

A

Marker	BSR4	BAG1	GRA6	ROP1	SAG3	# SO	% SO
Marker Type	Seq	Seq	Seq	RFLP	Seq		
Chromosome	IV	VIIb	X	XI	XII		
Length	1138	1917	758	Dde1	253		
Type I							
Type II							
Type III							
II						14	26
A	32	44	44			19	36
B	32	44	32	32		4	7.5
C	32	32	32			5	9.4
D	32	44	44			5	9.4
E	32	32	44			1	1.9
F	32	44	32			3	5.7
G				44		1	1.9
H	32	44				1	1.9

B

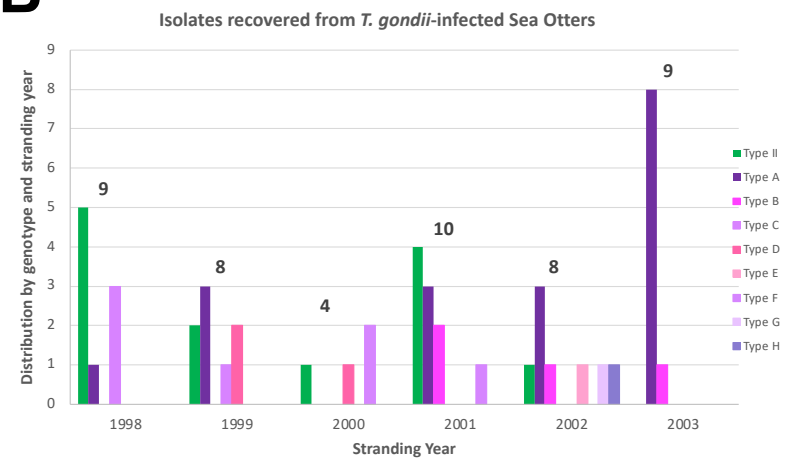

C

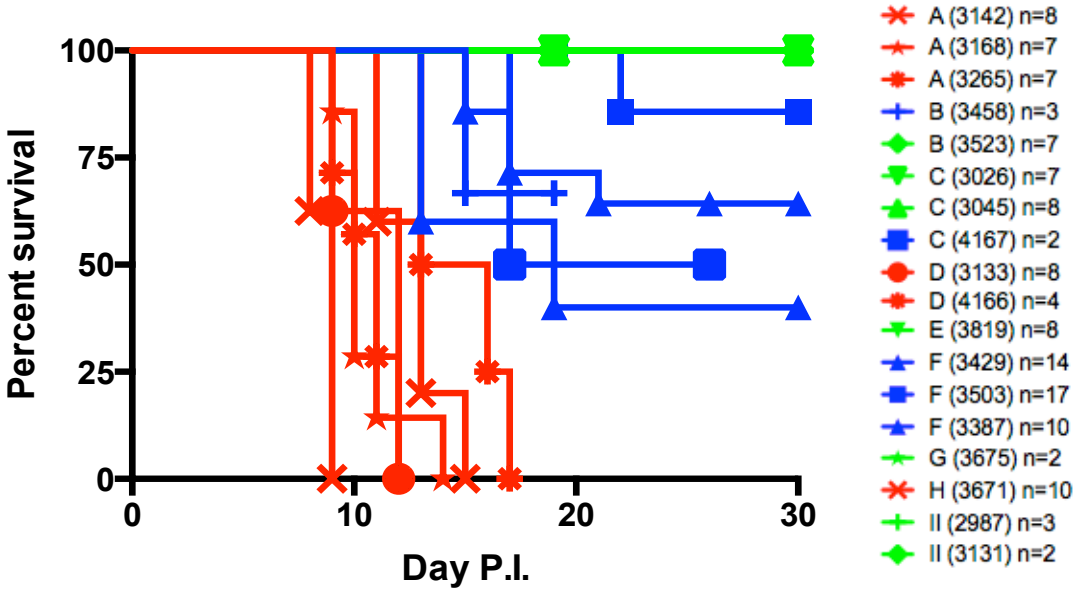

D

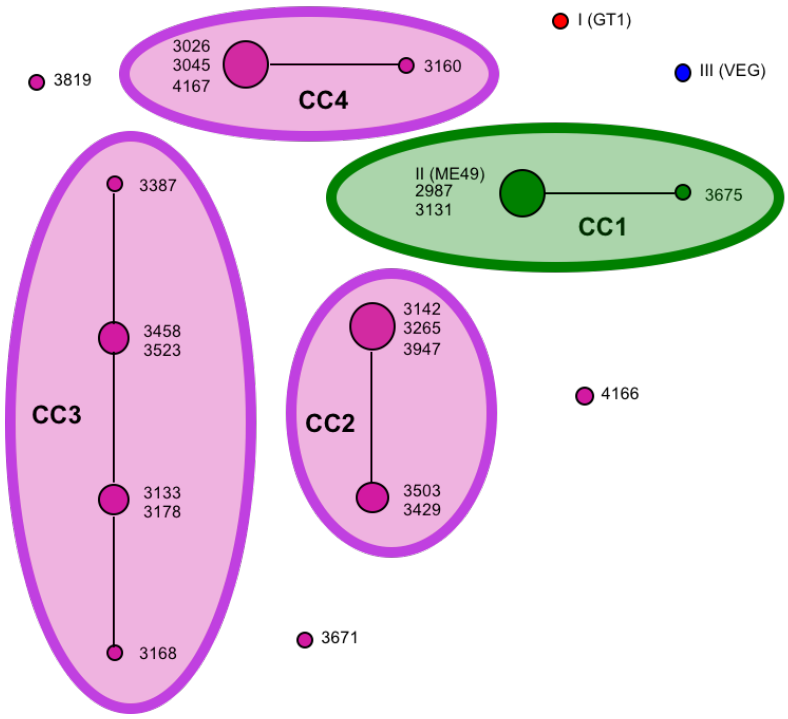

Figure 1_Kennard

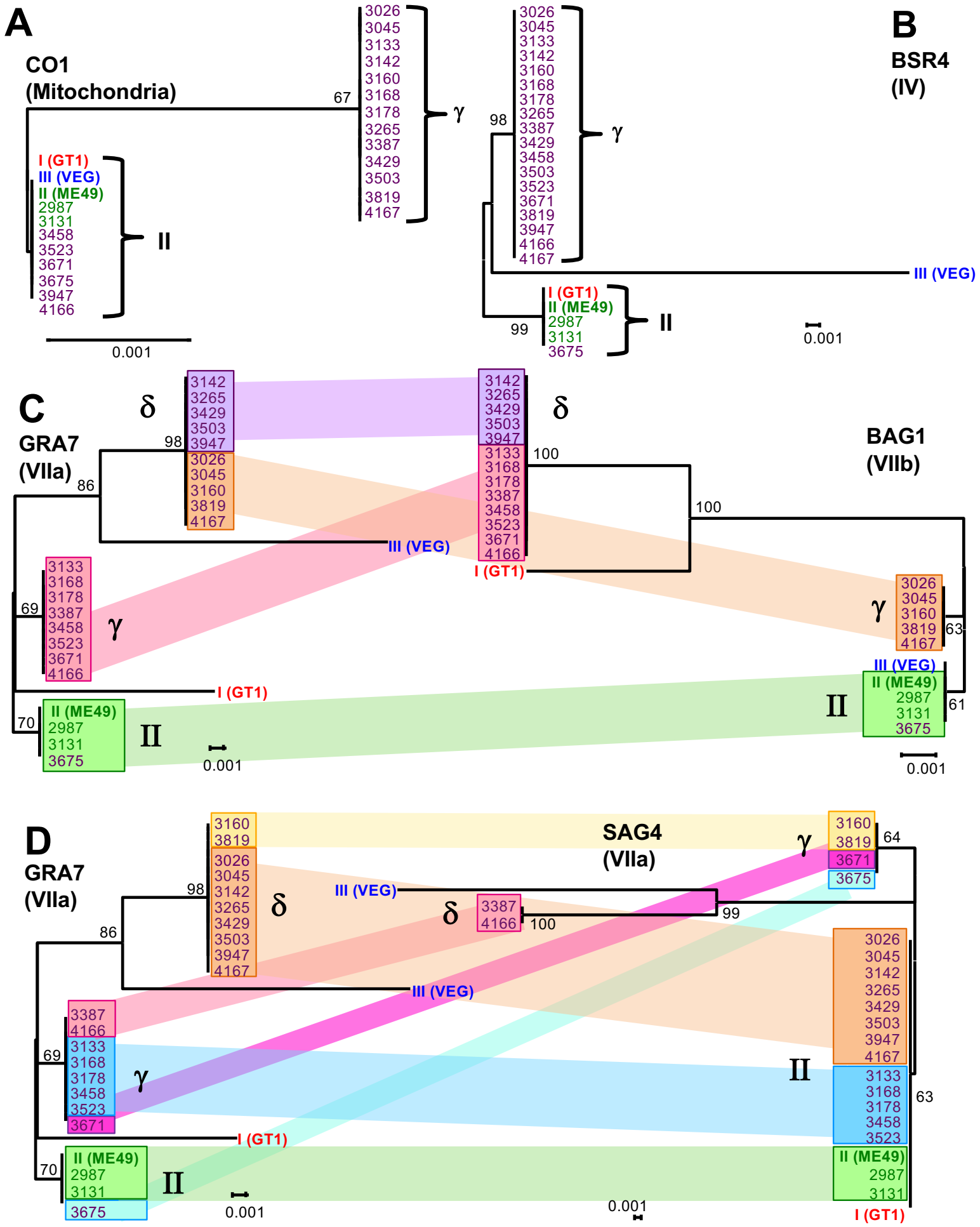

Figure 2_Kennard

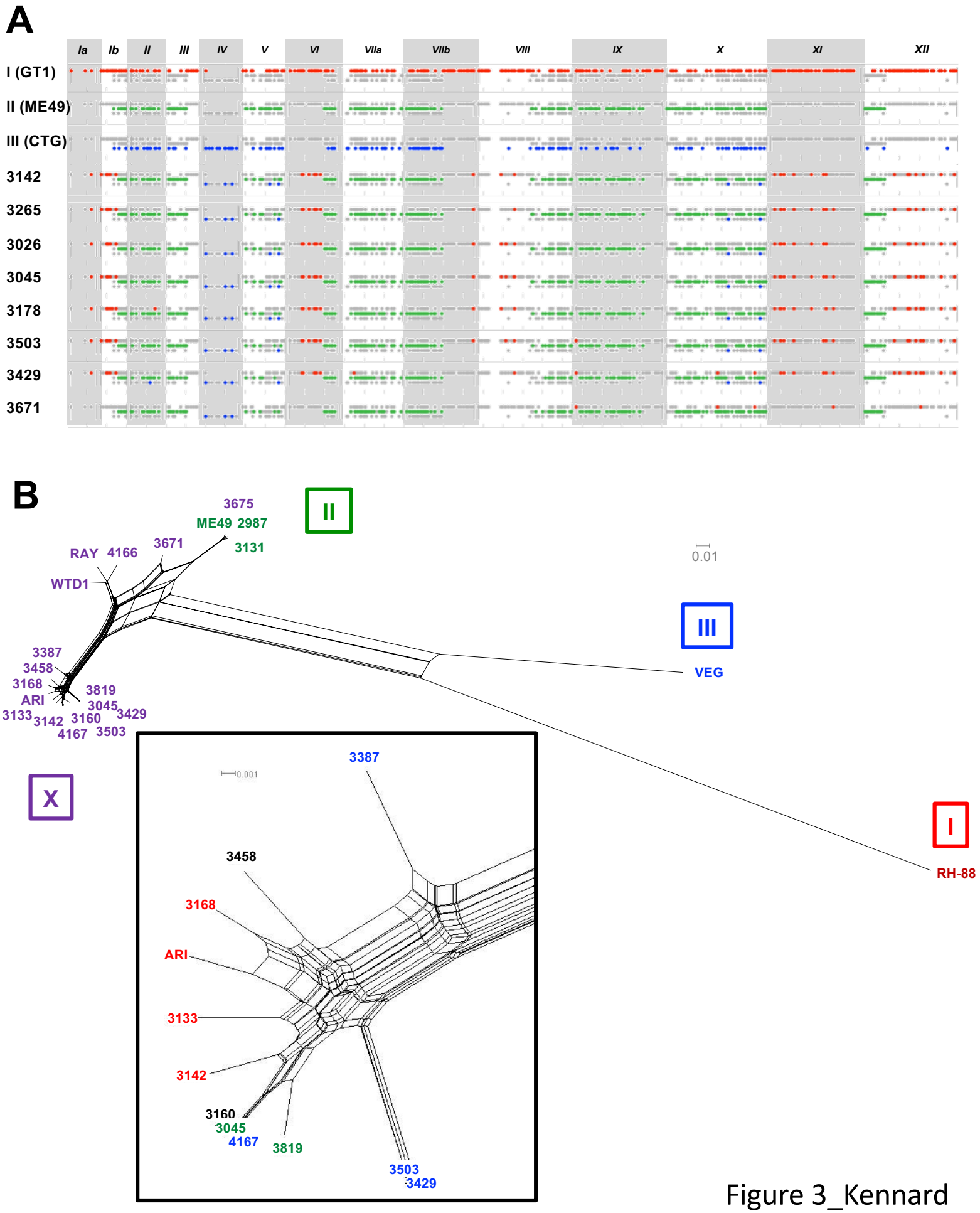

Figure 3_Kennard

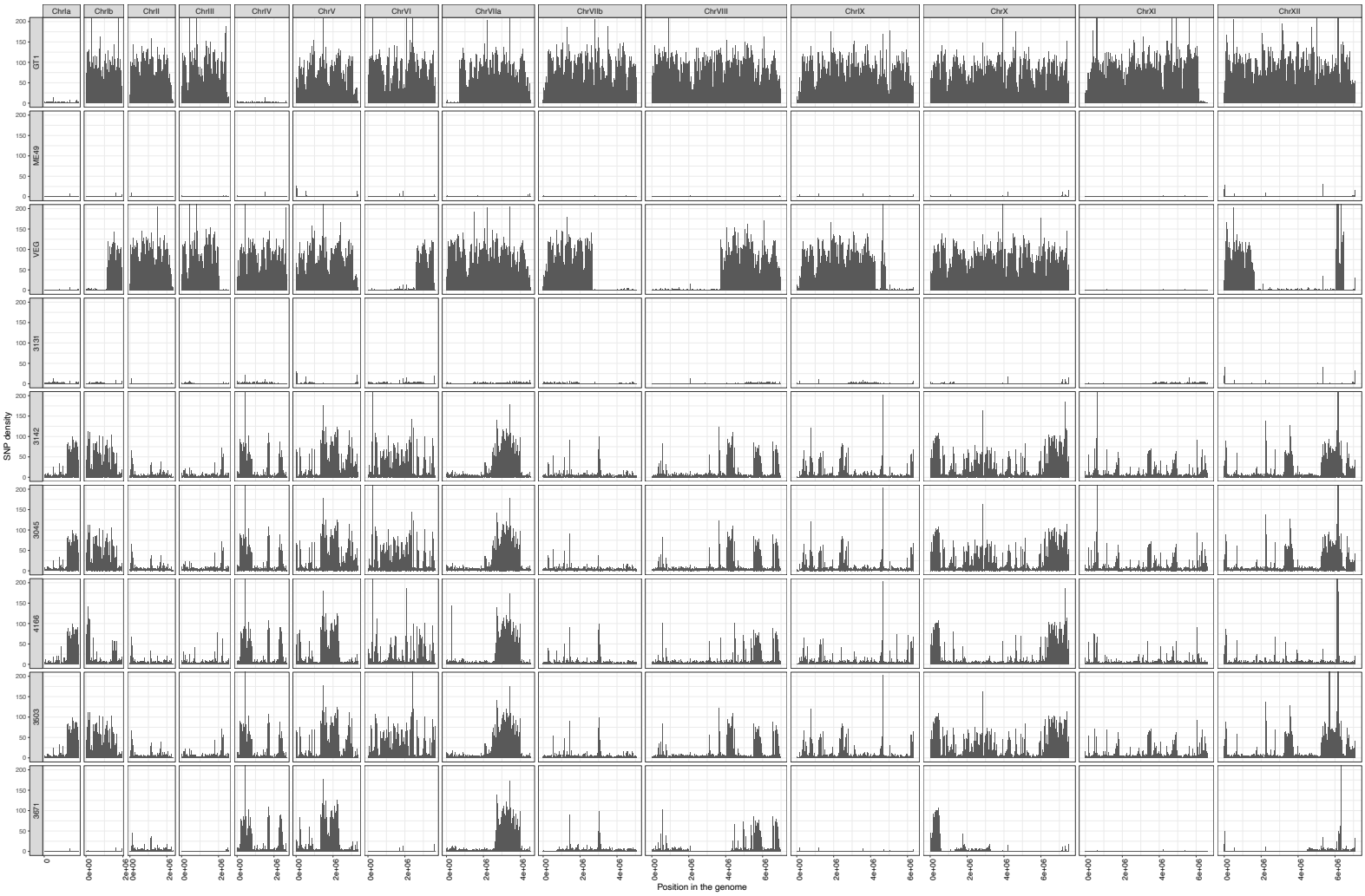

Figure 4_Kennard

A

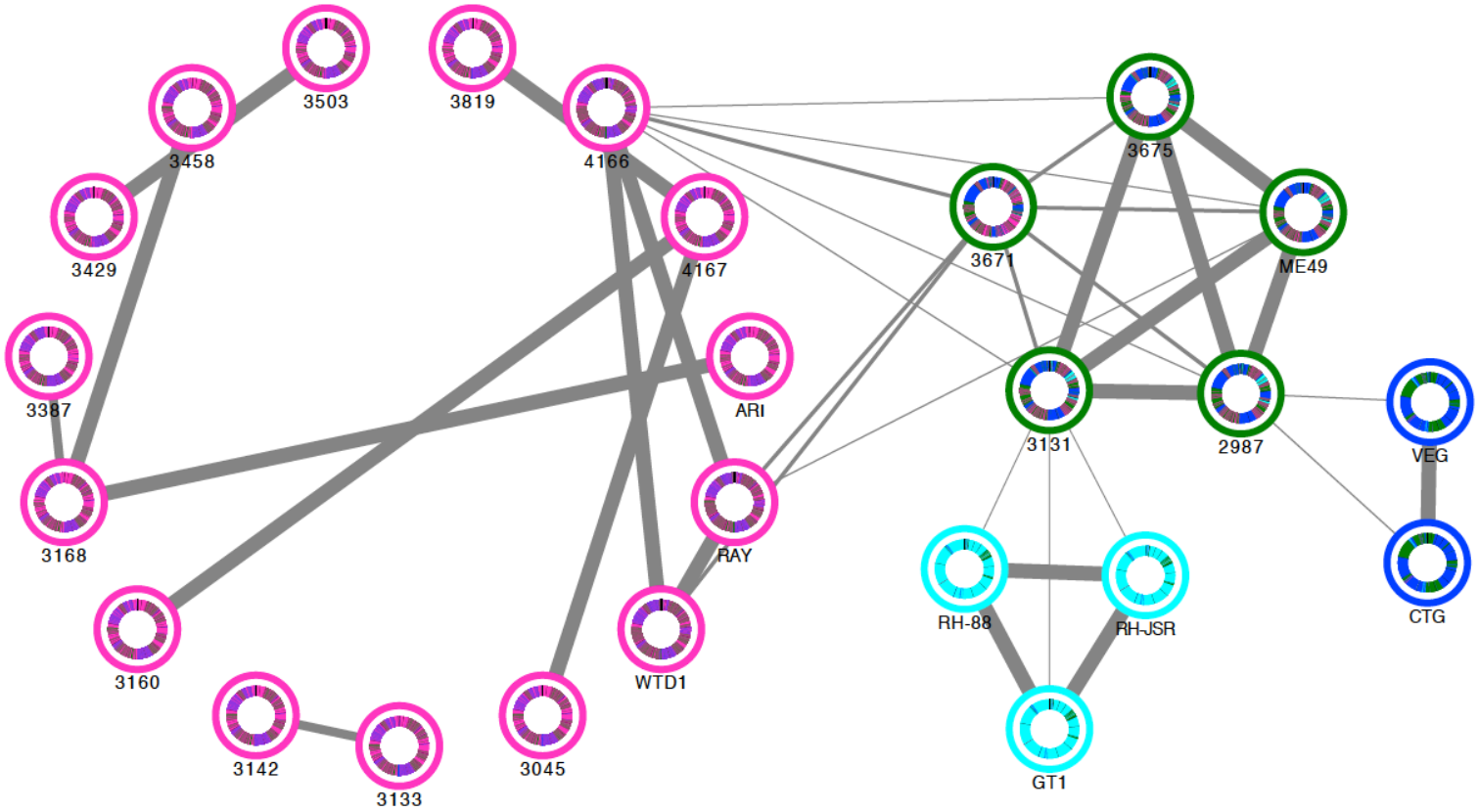

B

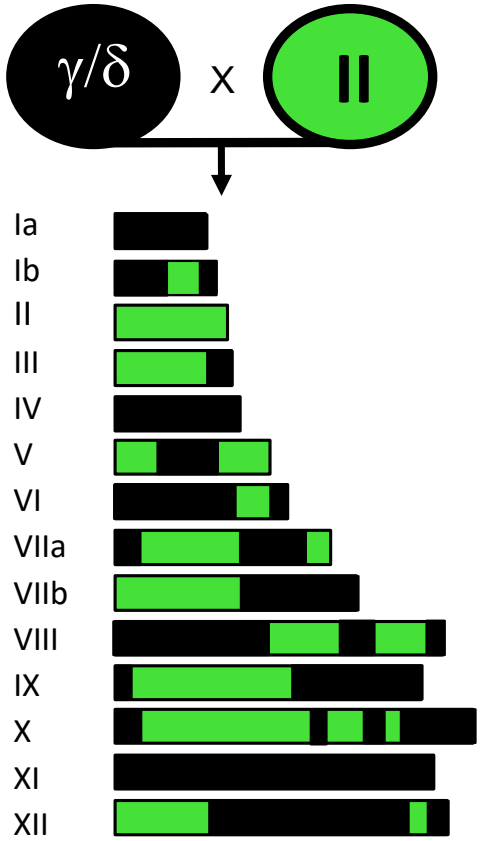

C

Isolate	CC	5 loci	17 loci	WGS	Mice	Otter
2987	CC1	II	II	II	-	+/-
3131	CC1	II	II	II	-	-
3142	CC2	A	X1	X1	+	-
3265	CC2	A	X1	n.d.	+	-
3947	CC2	A	X1	X2	n.d.	-
3168	CC3	A	X2	X3	+	-
3458	CC3	B	X3	X4	+/-	+
3523	CC3	B	X3	X4	-	-
3026	CC4	C	X4	X5	-	-
3045	CC4	C	X4	X5	-	-
4167	CC4	C	X4	X5	+/-	+
3160	CC4	C	X5	X6	n.d.	-
3133	CC3	D	X6	X7	+	+/-
3178	CC3	D	X6	X8	n.d.	-
4166	-	D	X7	X9	+	+
3819	-	E	X8	X10	-	-
3503	CC2	F	X9	X11	+/-	+
3429	CC2	F	X9	X12	+/-	+
3387	CC3	F	X10	X13	+/-	+/-
3675	CC1	G	X11	X14	-	+/-
3671	-	H	X12	X15	+	-

Figure 5_Kennard

A

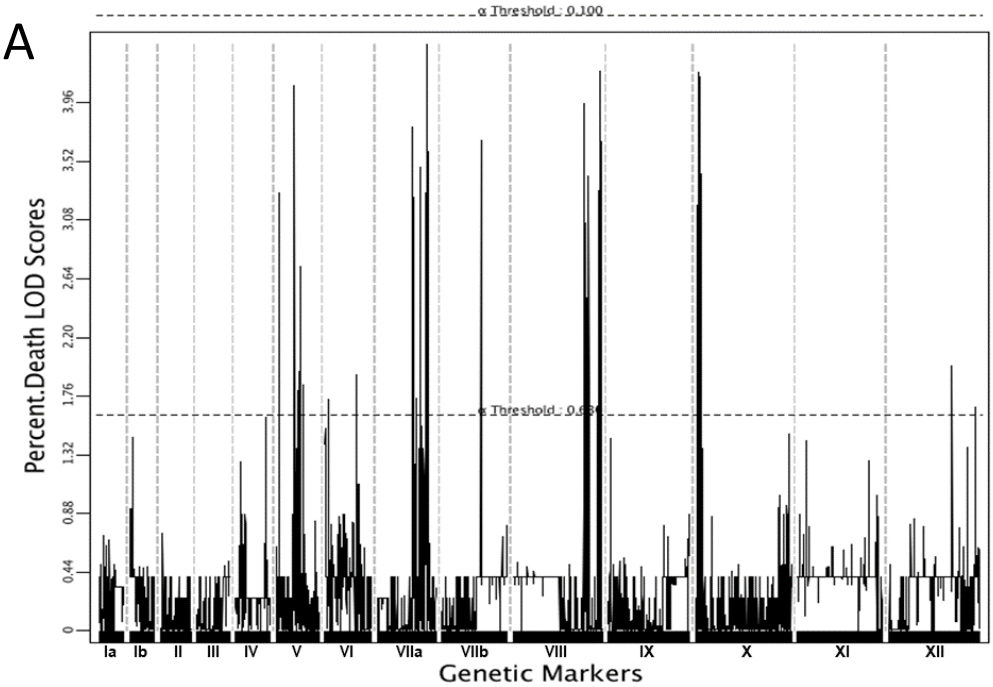

B

Chrm	Start (bp)	End (bp)	LOD
V	1430036	2165042	4.091
VIIa	3815011	4085005	4.400
VIIb	3035265	3160030	3.680
VIII	6745008	6905157	4.194
X	7314	290066	4.190

C

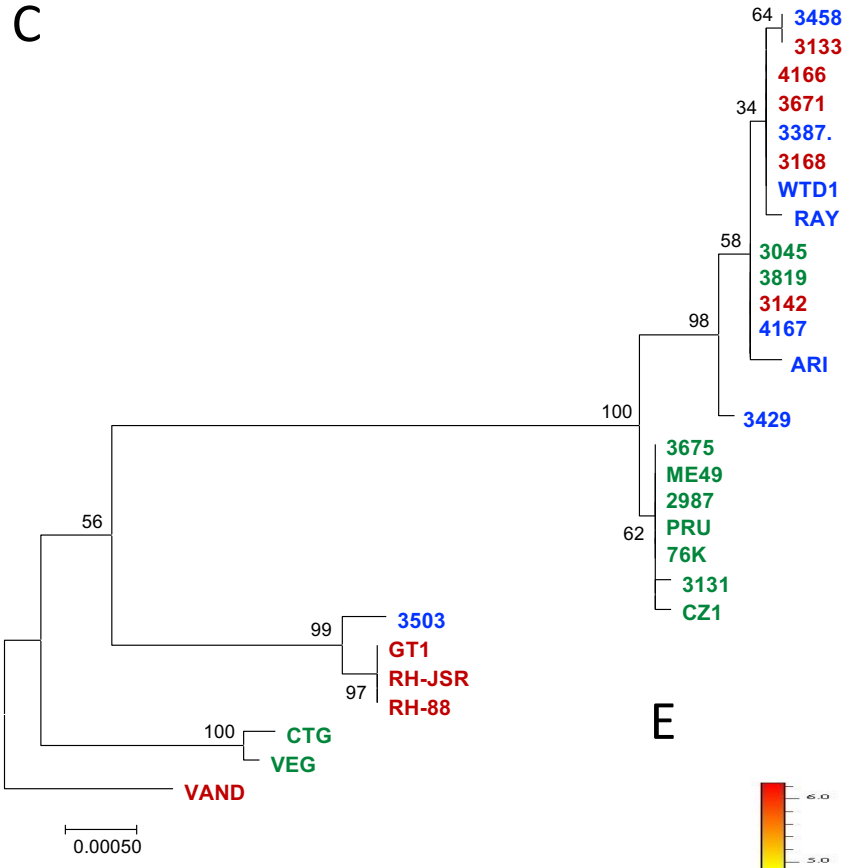

D

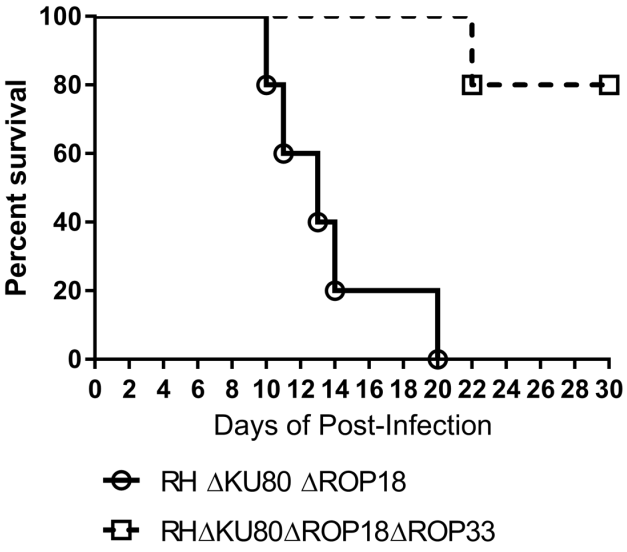

E

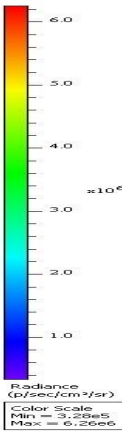

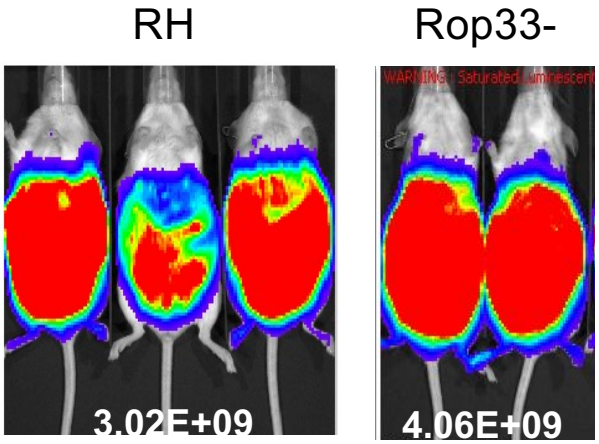

Figure 6_Kennard

A

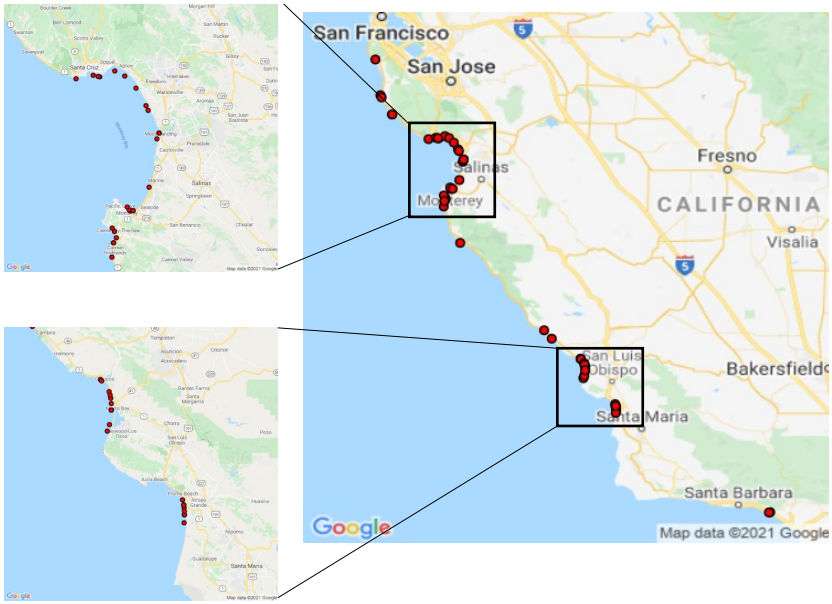

B

Sea otter and isolate #	ATOS #	5 loci	WGS	Lat	Long	Stranding Location	Necropsy Date	Sex	IFAT	Infection	Mouse virulence	SO virulence
3097	84	A		37.482	-122.461	Dunes Beach, San Mateo	11/16/98	M	5120	Tg		High
3786	180	A		37.111	-122.334	Ano Nuevo State Park	09/20/02	M	2560	Sn/Tg		Low
2922 (prev 3142)*	180	A	X1	37.111	-122.334	Ano Nuevo State Park	02/24/99	F	320	Sn/Tg	High	Low
4045	260	A		36.953	-122.003	Seabright Beach	10/21/03	M	10240	Tg		Low
3950	263	A		36.95	-121.987	21st Ave Beach, Santa Cruz	07/16/03	M	10240	Sn/Tg		Medium
3520*	306	A		36.863	-121.827	Sunset State Beach	05/16/01	M	320	Tg		Medium
3659	374	A		36.606	-121.875	Del Monte Beach	02/28/02	F	40	Tg		Low
3265	425	A		36.552	-121.935	Carmel Beach	09/28/99	F	10240	Tg	High	Low
3865	430	A		36.536	-121.929	Carmel River State Beach	04/03/03	F	10240	Sn/Tg		Low
3168	450	A	X3	36.486	-121.943	Yankee Point Cove	04/09/99	F	2560	Tg	High	Low
3947	523	A	X2	36.237	-121.818	Pfieffer Burns Beach	06/26/03	F	20480	Tg	n.d.	Low
4003	750	A		35.579	-121.123	Cambria	09/17/03	F	10240	Tg		Low
4071	807	A		35.441	-120.905	Cayucos State Beach	12/03/03	F	2560	Sn/Tg		Low
3483	820	A		35.392	-120.872	Morro Strand State Beach	03/30/01	F	320	Tg		Low
4151	827	A		35.361	-120.87	Morro Bay Harbor	4/9/04	F	40960	Sn/Tg		High
3488	919	A		35.126	-120.642	Pismo State Beach	04/04/01	F	640	Sn/Tg		Low
3821	922	A		35.113	-120.638	Pismo State Beach	01/06/03	M	2560	Sn/Tg		Medium
3744	924	A		35.105	-120.637	Pismo State Beach	07/02/02	F	5120	Tg		Low
3637*	926	A		35.096	-120.636	Oceano Dunes	02/14/03	F	10240	Sn/Tg		Low
3523	141	B	X4	37.241	-122.423	Pescadero Point	05/31/01	F	5120	Sn/Tg	Low	Low
3458	422	B	X4	36.561	-121.942	Stillwater Cove	01/16/01	F	640	Tg	Medium	High
3897	435	B		36.523	-121.938	Pt Lobos State Reserve	04/22/03	F	10240	Tg		Low
3728	1445	B		34.373	-119.466	Pt. Mugu State Park, Ventura	05/29/02	M	320	Tg		Low
3077	145	C		37.226	-122.414	Bean Hollow, San Mateo	09/27/98	M	1280	Sn/Tg		Low
3045	808	C	X5	35.437	-120.901	Cayucos State Beach	07/09/98	F	no serum	Tg	Low	Low
4167	823	C	X5	35.378	-120.87	Morro Strand State Beach	4/12/04	M	10240	Sn/Tg	Medium	High
3026	840	C	X5	35.306	-120.883	Morro Bay Sandspit	06/24/98	M	320	Tg	Low	Low
3160	933	C	X6	35.066	-120.637	Pismo State Beach	03/29/99	M	320	Sn/Tg	n.d.	Low
3178*	321	D	X8	36.805	-121.792	Moss Landing Harbor	03/26/02	F	320	Sn/Tg	n.d.	Low
3183	816	D		35.409	-120.877	Morro Strand State Beach	05/04/99	F	640	Tg		Medium
3133*	818	D	X7	35.4	-120.874	Morro Strand State Beach	02/04/99	M	20480	Tg	High	Medium
4166	827	D	X9	35.361	-120.87	Morro Bay	4/13/04	M	40960	Sn/Tg	High	High
3451	836	D		35.323	-120.876	Morro Bay Sandspit	11/29/00	M	640	Tg		Low
3819*	732	E	X10	35.637	-121.181	San Simeon Bay	12/28/02	F	5120	Sn/Tg	Low	Low
3429*	827	F	X12	35.361	-120.87	Morro Bay	10/30/00	F	10240	Tg	Medium	High
3387	922	F	X13	35.113	-120.638	Pismo State Beach	07/19/00	F	20480	Tg	Medium	Medium
3503*	1319	F	X11	34.371	-119.475	Rincon Pt, Ventura	08/09/01	M	40960	Tg	Medium	High
3675	435	G	X14	36.523	-121.938	Point Lobos	03/20/02	F	1280	Sn/Tg	Low	Medium
3671	321	H	X15	36.805	-121.792	Elkhorn Slough	3/14/02	M	640	Sn/Tg	High	Low
2994*	249	II		36.944	-122.058	Natural Bridges State Beach	05/15/98	M	no serum	Sn/Tg		Low
3739	264	II		36.949	-121.982	26th Ave Beach, Santa Cruz	06/12/02	M	2560	Sn/Tg		Low
3576	274	II		36.964	-121.934	New Brighton State Beach	09/05/01	M	20480	Tg		Medium
3587	281	II		36.951	-121.902	Rio Del Mar Beach	09/22/01	M	1280	Sn/Tg		Medium
2987	291	II	II	36.92	-121.866	Manresa State Beach	05/11/98	F	1280	Sn/Tg	Low	Medium
4181*	303	II		36.875	-121.834	Sunset State Beach	04/16/04	F	40960	Sn/Tg		Low
3009	321	II		36.805	-121.792	Elkhorn Slough	06/04/98	M	640	Tg		Low
3521	325	II		36.79	-121.799	Salinas River State Beach	05/19/01	M	2560	Tg		Medium
3208	356	II		36.666	-121.824	Monterey Bay	07/12/99	M	5120	Sn/Tg		Low
3636	376	II		36.605	-121.884	Del Monte Beach	12/27/01	M	80	Sn/Tg		Low
3087	377	II		36.608	-121.888	Monterey Harbor	10/28/98	F	640	Sn/Tg		Low
3131	379	II	II	36.615	-121.894	Monterey Bay	02/05/99	M	320	Tg	Low	Low
3005	928	II		35.087	-120.636	Pismo State Beach	06/01/98	M	160	Sn/Tg		Low
3396*	928	II		35.087	-120.636	Oceano Dunes	11/11/00	M	81920	Tg		High
		n=53	n=21									

* Tg strains isolated from sea otters not included in study from Shapiro et al, 2019

Supplemental Figure 1

Marker	5 Loci	17 Loci	C228	Chr_II_10	C292	BSR4	L358	PK1	SAG4	ROP18	GRA7	BAG1	SRS2	SAG1	SAG2	BTB	GRA6	ROP1	UPRT	SAG3	APICO	COX1
Chromosome			Ib	II	III	IV	V	VI	VIIa	VIIa	VIIa	VIIb	VIII	VIII	VIII	IX	X	XI	XI	XII	API	MITO
Length			421	639	397	1138	354	1011	174	1617	460	1917	983	700	1243	331	758	960	1214	253	442	418
Type I		I	α	α	α	Type II	α	Type II	Type II	Type II	Type II	Type II	Type II	Type II	Type II	Type II	Type II	Type II	Type II	α	α	Type II
Type II		II	Type II	Type II	Type II	Type II	Type II	Type II	Type II	Type II	Type II	Type II	Type II	Type II	Type II	Type II	Type II	Type II	Type II	Type II	Type II	Type II
Type III		III	β	β	β	β	β	β	Type II	β	β	Type II	Type II	Type II	β	β	β	Type II	Type II	β	β	Type II
2987	II	II	Type II	Type II	Type II	Type II	Type II	Type II	Type II	Type II	Type II	Type II	Type II	Type II	Type II	Type II	Type II	Type II	Type II	Type II	α	Type II
3131	II	II	Type II	Type II	Type II	Type II	Type II	44	Type II	Type II	Type II	Type II	Type II	Type II	Type II	Type II	Type II	Type II	Type II	Type II	Type II	Type II
3142	A	X1	Type II	Type II	Type II	32	α	44	Type II	32	44	44	32	32	Type II	32	44	32	Type II	Type II	α	32
3265	A	X1	Type II		Type II	32	α	44	Type II	32	44	44	32	32	Type II	32	44	32		Type II	α	32
3947	A	X1	Type II			32	α	44	Type II	32	44	44	32	32	Type II	32	44	44		Type II	α	
3168	A	X2	Type II	Type II	Type II	32	α	Type II	Type II	32	32	44	32	32	Type II	32	44	44	Type II	Type II	α	32
3458	B	X3	Type II	Type II	Type II	32	α	32	Type II	32	32	44	32	32	Type II	32	32	γ	Type II	Type II	32	Type II
3523	B	X3	Type II		Type II	32	α	32	Type II	32	32	44	32	32	Type II	32	32	γ	Type II	Type II	32	Type II
4167	C	X4	Type II	Type II	Type II	32	α	44	Type II	44	44	32	32	32	Type II	32	32	32	Type II	Type II	α	32
3026	C	X4	Type II	Type II	Type II	32	α	44	Type II	44	44	32	32	32	Type II	32	32	32	Type II	Type II	α	32
3045	C	X4	Type II	Type II	Type II	32	α	44	Type II	44	44	32	32	32	Type II	32	32	32	Type II	Type II	α	32
3160	C	X5	Type II	Type II	Type II	32	α	44	32	44	44	32	32	32	Type II	32	32	32	Type II	Type II	α	32
3133	D	X6	Type II	Type II	Type II	32	α	32	Type II	32	32	44	32	32	Type II	32	44	Type II	Type II	Type II	α	32
3178	D	X6	Type II	Type II	Type II	32	α	32	Type II	32	32	44	32	32	Type II	32	44	Type II	Type II	Type II	α	32
4166	D	X7	Type II	Type II	Type II	32	α	44	44	32	32	44	32	32	Type II	32	44	γ	Type II	Type II	α	Type II
3819	E	X8	Type II	Type II	Type II	32	α	44	32	32	44	32	32	32	Type II	32	44	Type II	Type II	Type II	α	32
3503	F	X9	Type II	Type II	Type II	32	α	44	Type II	32	44	44	32	32	Type II	32	32	32	Type II	Type II	α	32
3429	F	X9	Type II	Type II	Type II	32	α	44	Type II	32	44	44	32	32	Type II	32	32	32	Type II	Type II	Type II	32
3387	F	X10	Type II	Type II	Type II	32	32	32	44	32	32	44	32	32	Type II	32	32	44	Type II	Type II	α	32
3675	G	X11	Type II	Type II	Type II	Type II	Type II	Type II	32	Type II	Type II	Type II	Type II	Type II	Type II	Type II	Type II	γ	Type II	Type II	α	Type II
3671	H	X12	Type II	Type II	Type II	32	α	Type II	32	32	32	44	Type II	Type II	Type II	Type II	Type II	Type II	Type II	Type II	α	Type II

Type II	Type II
α	α
β	β
γ	32
δ	44

Supplemental Table 1

Chr	Start (bp)	End (bp)	LOD	TM	Signal	Gene ID	Genomic Location(s)	Product Description
5	220001	350021	3.25	Y	Y	TGME49_220240	TGME49_chrV:235,019..240,463(-)	hypothetical protein
				Y	Y	TGME49_220300	TGME49_chrV:275,453..283,005(-)	ribosomal protein L15 protein
				Y	Y	TGME49_220330	TGME49_chrV:295,153..299,369(-)	hypothetical protein
				Y	Y	TGME49_220350	TGME49_chrV:310,715..318,211(+)	tRNA ligases class II (D, K and N) domain-containing protein
5	1430036	2165042	4.09	Y	Y	TGME49_285870	TGME49_chrV:2,158,544..2,162,541(-)	SAG-related sequence SRS20A
				Y	Y	TGME49_285940	TGME49_chrV:2,123,872..2,135,543(-)	hypothetical protein
				Y	Y	TGME49_286180	TGME49_chrV:1,933,873..1,942,288(-)	tRNA ligases class I (M) protein
				Y	Y	TGME49_286450	TGME49_chrV:1,824,587..1,826,598(+)	dense granule protein GRA5
				Y	Y	TGME49_286530	TGME49_chrV:1,790,919..1,793,716(+)	hypothetical protein
				Y	Y	TGME49_286620	TGME49_chrV:1,754,511..1,762,820(-)	S1 RNA binding domain-containing protein
				Y	Y	TGME49_286630	TGME49_chrV:1,750,888..1,752,970(+)	redoxin domain-containing protein
				Y	Y	TGME49_286770	TGME49_chrV:1,682,413..1,683,569(+)	hypothetical protein
				Y	Y	TGME49_213920	TGME49_chrV:1,428,849..1,440,483(-)	hypothetical protein
7a	3815011	4085005	4.40	Y	Y	TGME49_201130	TGME49_chrVIIa:4,019,644..4,026,659(+)	rhoptry kinase family protein ROP33
				Y	Y	TGME49_201180	TGME49_chrVIIa:3,982,746..3,988,716(-)	hypothetical protein
				Y	Y	TGME49_201390	TGME49_chrVIIa:3,908,769..3,911,287(-)	hypothetical protein
				Y	Y	TGME49_201750	TGME49_chrVIIa: 3,822,835 – 3,823,206(+)	Tctex-1 family protein
				Y	Y	TGME49_201760	TGME49_chrVIIa: 3,816,484 – 3,820,369(+)	hypothetical protein
7b	3035265	3160030	3.68	Y	Y	TGME49_258828	TGME49_chrVIIb:3,159,970..3,160,907(+)	hypothetical protein
				Y	Y	TGME49_258840	TGME49_chrVIIb:3,137,682..3,141,698(+)	hypothetical protein
				Y	Y	TGME49_258860	TGME49_chrVIIb:3,122,191..3,126,503(+)	hypothetical protein
				Y	Y	TGME49_258890	TGME49_chrVIIb:3,103,220..3,104,003(-)	hypothetical protein
				Y	Y	TGME49_258910	TGME49_chrVIIb:3,092,653..3,098,081(+)	hypothetical protein
				Y	Y	TGME49_258950	TGME49_chrVIIb:3,079,180..3,083,732(+)	lectin family protein
				Y	Y	TGME49_258990	TGME49_chrVIIb:3,038,025..3,049,513(+)	Bromodomain-containing protein
				Y	Y	TGME49_259000	TGME49_chrVIIb:3,035,953..3,049,513(+)	hypothetical protein
8	5435051	6125010	3.8	Y	Y	TGME49_269150	TGME49_chrVIII:6,039,099..6,042,614(-)	DHHC zinc finger domain-containing protein
				Y	Y	TGME49_269190	TGME49_chrVIII:6,002,854..6,007,557(-)	glyceraldehyde-3-phosphate dehydrogenase GAPDH2
				Y	Y	TGME49_269400	TGME49_chrVIII:5,836,645..5,840,235(+)	oxidoreductase, short chain dehydrogenase/reductase family protein
				Y	Y	TGME49_269750	TGME49_chrVIII:5,625,999..5,628,567(+)	CrcB family protein
				Y	Y	TGME49_269885	TGME49_chrVIII:5,564,529..5,572,853(+)	rhoptry metalloprotease toxolysin TLN1
				Y	Y	TGME49_269920	TGME49_chrVIII:5,535,689..5,545,827(-)	phosphatidylserine decarboxylase
				Y	Y	TGME49_269980	TGME49_chrVIII:5,483,536..5,489,390(-)	preprotein translocase Sec61, putative
				Y	Y	TGME49_269690	TGME49_chrVIII:5,680,572..5,684,829(+)	hypothetical protein
				Y	Y	TGME49_270030	TGME49_chrVIII:5,448,751..5,449,486(+)	hypothetical protein
8	6745008	6905157	4.19	Y	Y	TGME49_200230	TGME49_chrVIII:6,753,611..6,755,422(-)	microneme protein MIC17C
				Y	Y	TGME49_200440	TGME49_chrVIII:6,883,172..6,887,049(+)	hypothetical protein
10	280002	290066	4.19	N/A	N/A	N/A	N/A	N/A

Supplemental Table 2